

Auxiliary materials

Evaluating Inter-Continental Transport of Fine Aerosols: (1) Methodology, Global Aerosol Distribution and Optical Depth

Junfeng Liu^{1,2}, Denise Mauzerall¹, Larry Horowitz³, Paul Ginoux³, and Arlene Fiore³

[1] Woodrow Wilson School, Princeton University, Princeton, NJ 08544

[2] Now at: Geophysical Fluid Dynamics Laboratory, Princeton, NJ 08540

[3] Geophysical Fluid Dynamics Laboratory, Princeton, NJ 08540

Part-I Additional Tables and Figures

Table A1 Budget of annual average fine surface aerosol concentrations (SAC) (weighted by area; units: $\mu\text{g}\cdot\text{m}^{-3}$) from inter-continental transport (ITCT) of aerosols from each source region to each receptor region for ammonium sulfate, black carbon (BC), organic mass (OM= 1.3·OC1+1.7·OC2) and fine dust aerosols.

	Sources		Receptors									
	ITCT	Unit	NA	SA	EU	FSU	AF	IN	EA	SE	AU	ME
Sulfate	ITCT	$\mu\text{g}\cdot\text{m}^{-3}$	0.06	0.01	0.30	0.45	0.41	0.42	0.44	0.56	0.02	0.95
	NA	%	-	52	29	6	13	9	7	1	1	9
	SA	%	3	-	0	0	1	0	0	0	19	0
	EU	%	28	6	-	68	59	12	23	1	0	54
	FSU	%	9	0	23	-	0	6	34	0	0	8
	AF	%	2	19	14	1	-	6	1	0	70	22
	IN	%	3	2	0	2	2	-	19	11	1	5
	EA	%	49	5	4	10	3	6	-	84	2	2
	SE	%	1	4	0	0	0	2	4	-	8	0
	AU	%	0	11	0	0	0	0	0	1	-	0
ME	%	6	1	30	13	21	60	12	1	0	-	
BC	ITCT	$\mu\text{g}\cdot\text{m}^{-3}$	0.006	0.004	0.020	0.035	0.022	0.033	0.047	0.064	0.005	0.054
	NA	%	-	13	17	3	9	4	2	0	0	5
	SA	%	9	-	0	0	5	1	0	0	30	0
	EU	%	15	1	-	55	61	7	10	0	0	45
	FSU	%	8	0	17	-	0	2	28	0	0	3
	AF	%	7	78	21	1	-	16	2	1	59	29
	IN	%	6	1	1	4	5	-	37	27	0	13
	EA	%	52	1	6	25	5	10	-	66	1	3
	SE	%	3	3	0	0	1	15	15	-	9	1
	AU	%	0	4	0	0	0	0	0	5	-	0
ME	%	2	0	38	12	13	44	5	0	0	-	
OM	ITCT	$\mu\text{g}\cdot\text{m}^{-3}$	0.033	0.050	0.107	0.149	0.144	0.240	0.387	0.330	0.051	0.319
	NA	%	-	10	26	7	10	4	2	0	0	7
	SA	%	15	-	0	0	8	2	0	1	27	1
	EU	%	9	1	-	43	63	5	5	0	0	37
	FSU	%	22	0	24	-	1	2	42	0	0	4
	AF	%	12	84	14	2	-	23	2	3	66	34
	IN	%	6	0	1	6	5	-	29	36	0	14
	EA	%	29	0	3	30	2	7	-	47	0	2
	SE	%	5	2	1	0	2	20	17	-	6	1
	AU	%	0	3	0	0	0	0	0	12	-	0
ME	%	2	0	31	13	9	37	3	0	0	-	
Dust	ITCT	$\mu\text{g}\cdot\text{m}^{-3}$	0.44	0.47	1.40	0.68	0.66	5.82	1.31	0.66	0.13	8.43
	NA	%	-	0	1	1	1	0	1	0	0	0
	SA	%	0	-	0	0	2	0	0	0	19	0
	EU	%	0	0	-	0	0	0	0	0	0	0

FSU	%	3	0	21	-	4	5	19	2	1	15
AF	%	76	91	71	49	-	47	53	45	67	83
IN	%	1	0	0	2	2	-	6	4	1	1
EA	%	11	0	3	24	4	1	-	11	1	1
SE	%	0	0	0	0	0	0	0	-	0	0
AU	%	0	2	0	0	1	0	0	15	-	0
ME	%	9	5	5	25	85	46	22	23	11	-

Table A2 Same as Table A1, but for aerosol optical depth.

		Sources	Unit		Receptors								
			NA	SA	EU	FSU	AF	IN	EA	SE	AU	ME	
Sulfate	ITCT		0.0079	0.0014	0.018	0.030	0.0089	0.013	0.018	0.012	0.0023	0.021	
		NA	%	-	30	48	15	20	11	14	2	4	16
		SA	%	2	-	0	0	3	1	1	1	16	1
		EU	%	16	3	-	50	32	10	20	1	0	36
		FSU	%	5	0	9	-	1	5	16	0	0	5
		AF	%	2	12	7	2	-	5	3	1	34	15
		IN	%	8	6	3	2	9	-	25	15	4	12
		EA	%	56	23	17	18	12	20	-	77	16	13
		SE	%	5	17	2	1	5	8	7	-	25	3
		AU	%	0	7	0	0	0	0	0	1	-	0
	ME	%	6	1	15	12	18	40	15	2	1	-	
BC	ITCT		0.0016	0.0006	0.0020	0.0032	0.0015	0.0026	0.0032	0.0021	0.0013	0.0036	
		NA	%	-	11	26	9	10	5	5	1	1	7
		SA	%	10	-	5	3	25	7	4	4	29	5
		EU	%	6	1	-	36	20	4	8	0	0	18
		FSU	%	3	0	5	-	0	1	9	0	0	1
		AF	%	9	52	14	5	-	27	8	8	40	30
		IN	%	12	4	8	6	13	-	38	28	2	17
		EA	%	46	9	24	28	13	19	-	53	5	14
		SE	%	11	18	7	5	13	19	21	-	23	8
		AU	%	0	4	0	0	1	0	0	5	-	0
	ME	%	2	0	10	8	6	19	6	1	0	-	
OC	ITCT		0.0052	0.0028	0.0071	0.0084	0.0058	0.0104	0.014	0.0062	0.0064	0.014	
		NA	%	-	11	31	14	11	5	5	1	1	7
		SA	%	19	-	9	8	37	10	5	8	31	8
		EU	%	4	0	-	26	19	3	5	0	0	14
		FSU	%	10	0	8	-	1	1	16	0	0	2
		AF	%	15	63	17	10	-	40	11	16	48	42
		IN	%	12	3	7	7	10	-	30	32	1	14
		EA	%	24	3	12	20	6	8	-	31	1	6
		SE	%	14	14	9	7	12	19	24	-	17	8
		AU	%	1	5	0	0	1	0	0	10	-	0
	ME	%	2	0	6	7	4	14	4	1	0	-	
Dust	ITCT		0.0044	0.0051	0.0099	0.0064	0.0032	0.022	0.0088	0.0039	0.0016	0.026	
		NA	%	-	0	1	1	1	0	1	0	0	0
		SA	%	0	-	0	0	1	0	0	0	7	0
		EU	%	0	0	-	0	0	0	0	0	0	0
		FSU	%	4	1	6	-	5	4	10	2	1	9
		AF	%	67	88	80	63	-	52	61	55	73	88
		IN	%	2	1	1	1	5	-	5	6	2	2
		EA	%	13	1	5	14	5	1	-	5	2	1
		SE	%	0	0	0	0	0	0	0	-	0	0
		AU	%	1	3	0	0	3	0	0	9	-	0
	ME	%	13	7	7	20	79	42	23	24	15	-	

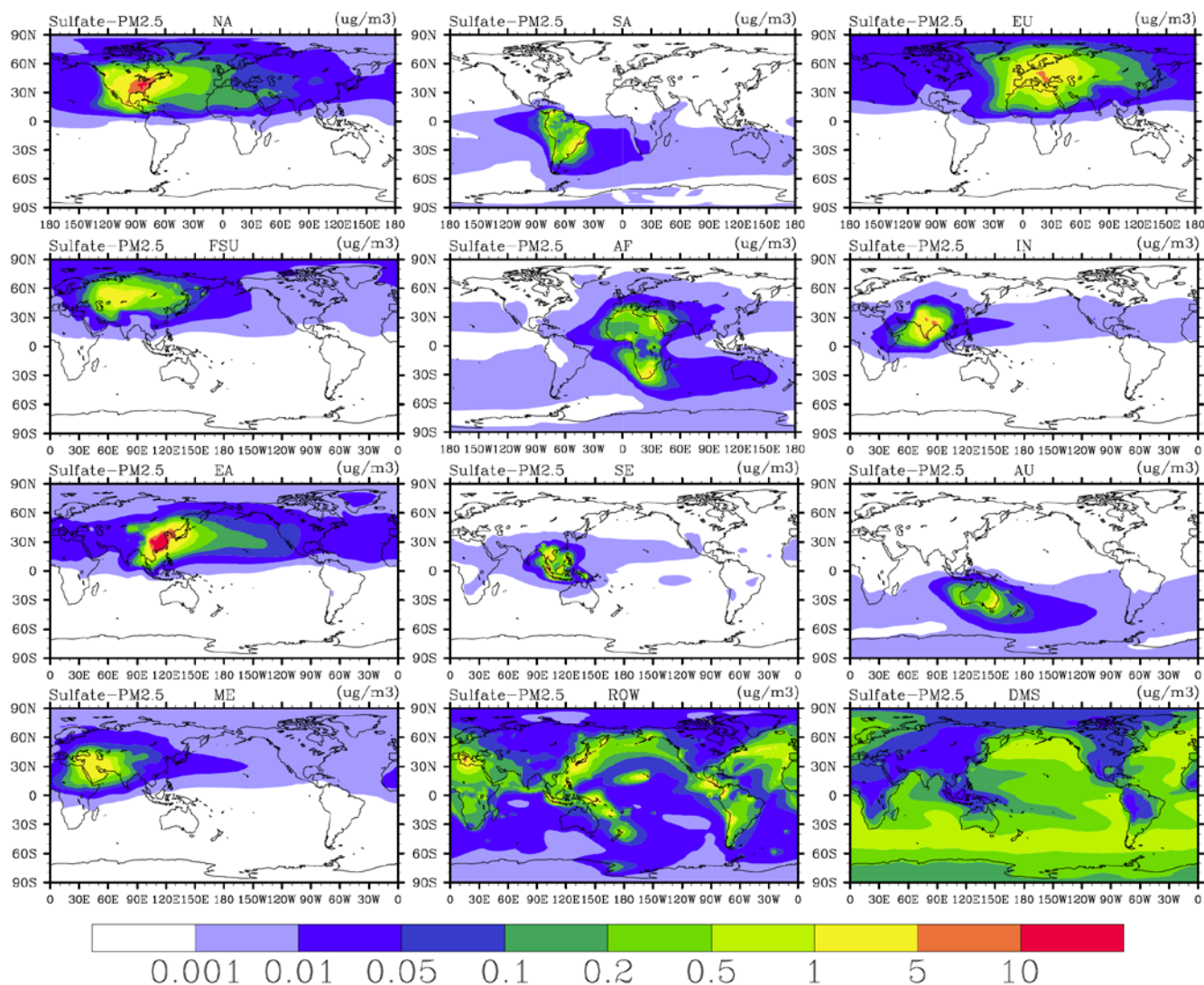


Figure A1 Simulated annual mean sulfate (i.e., ammonium sulfate) concentrations (PM2.5) at the surface (unit: $\mu\text{g}/\text{m}^3$) for each tagged tracer (note: regional tracers only represent anthropogenic emissions). ROW, rest of world, indicates emissions from ships, biomass burning and volcanoes. DMS indicates sulfate contributions from DMS oxidation.

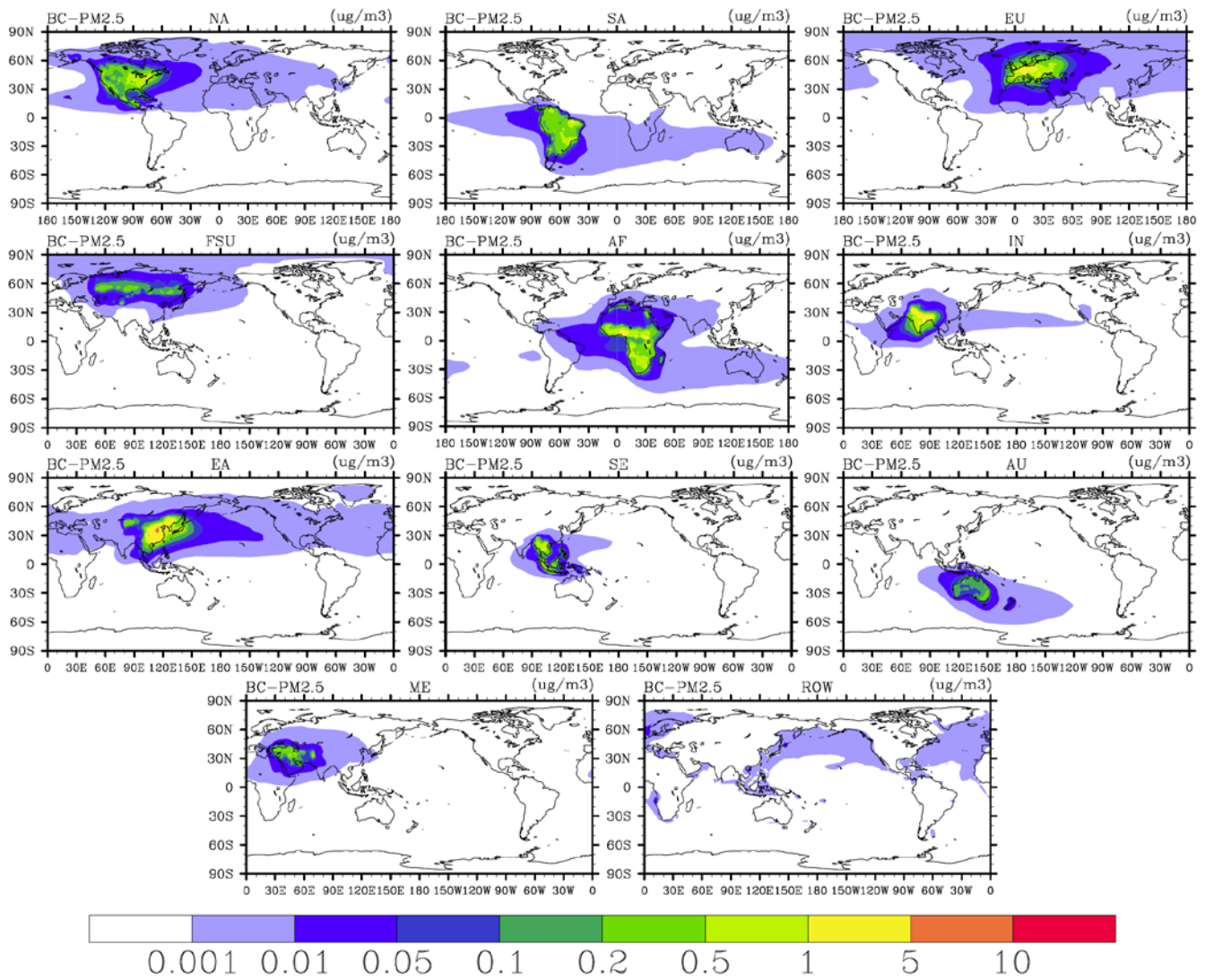


Figure A2 Same as Figure A1, but for black carbon aerosol tracers (Note: unlike sulfate tracers, each BC tracer tags both anthropogenic and biomass burning emissions)

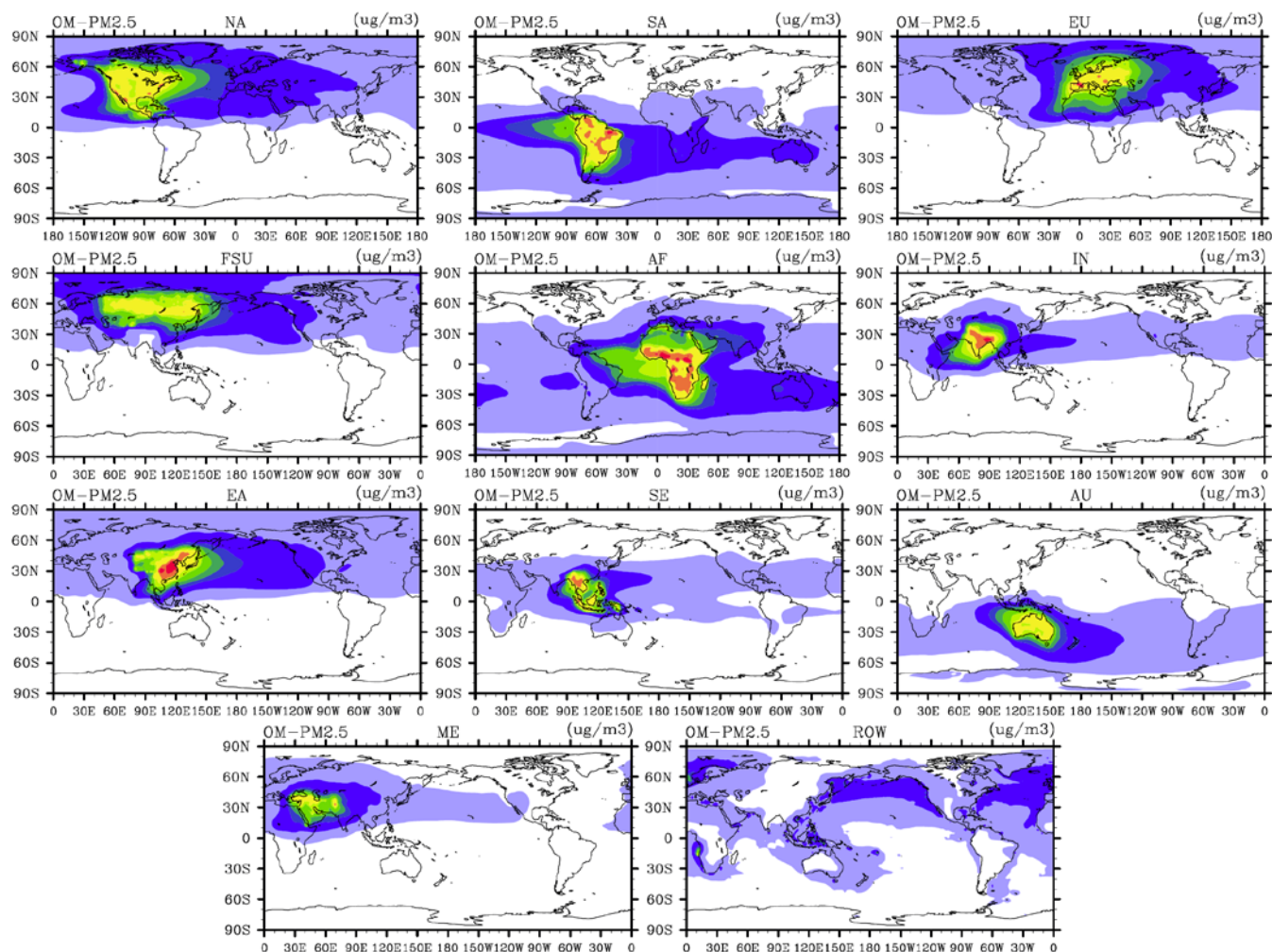


Figure A3 Same as Figure A2, but for organic mass (OM) aerosol tracers ($\text{OM} = 1.3 \cdot \text{OC1} + 1.7 \cdot \text{OC2}$; unit: $\mu\text{g m}^{-3}$). (Note: like BC tracers, each OC tracer tags both anthropogenic and biomass burning emissions).

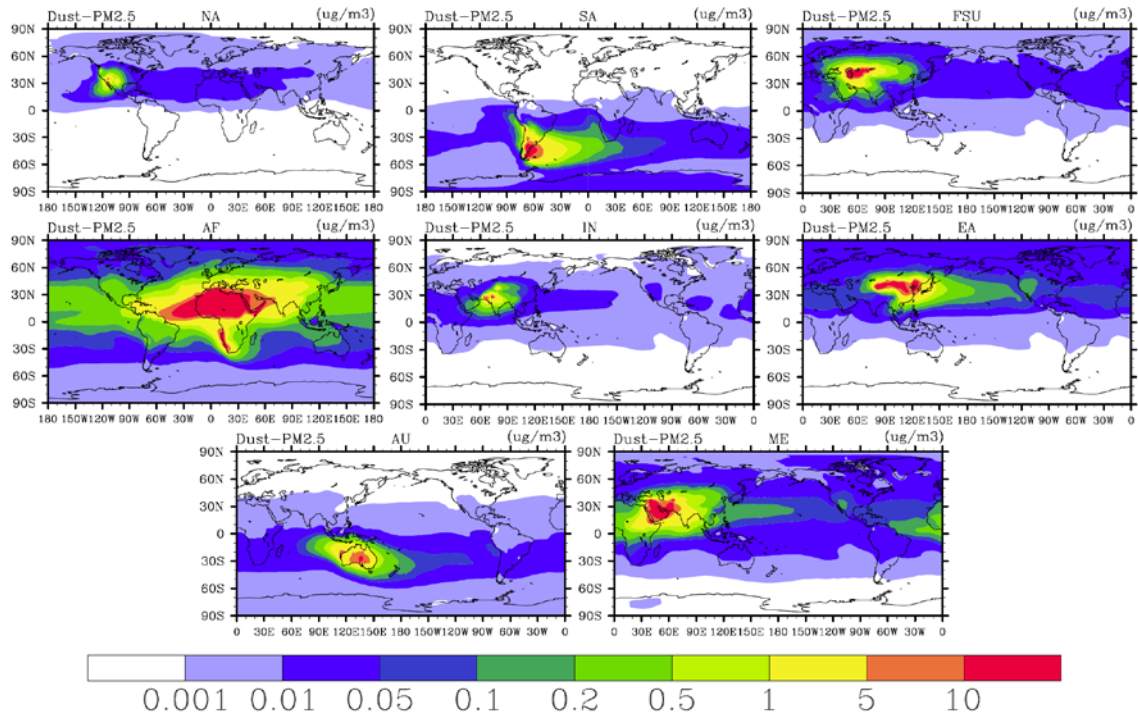


Figure A4 Same as Figure A1, but for fine dust (PM2.5) tracers (unit: $\mu\text{g}/\text{m}^3$).

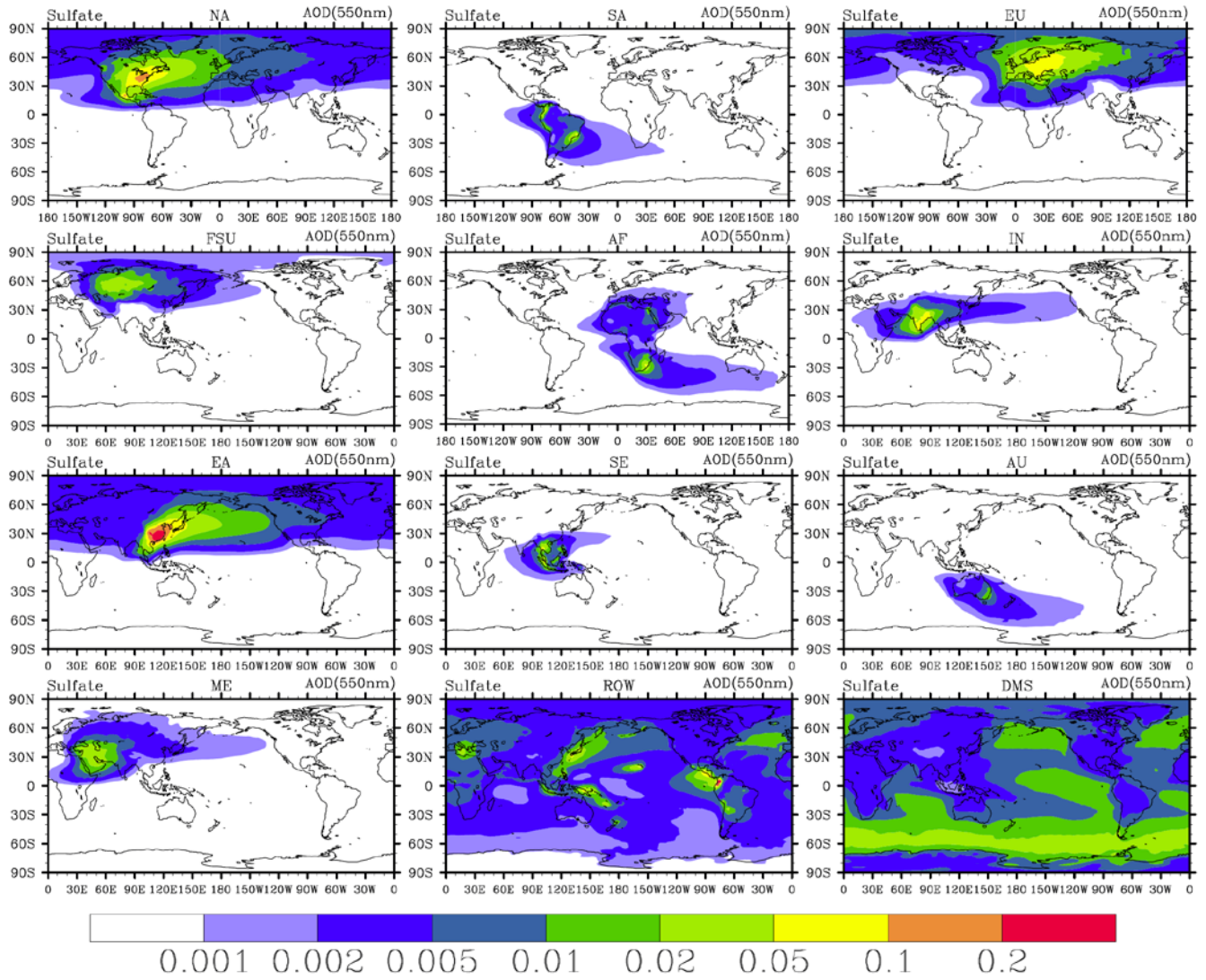


Figure A5 Same as Figure A1, but for sulfate AOD.

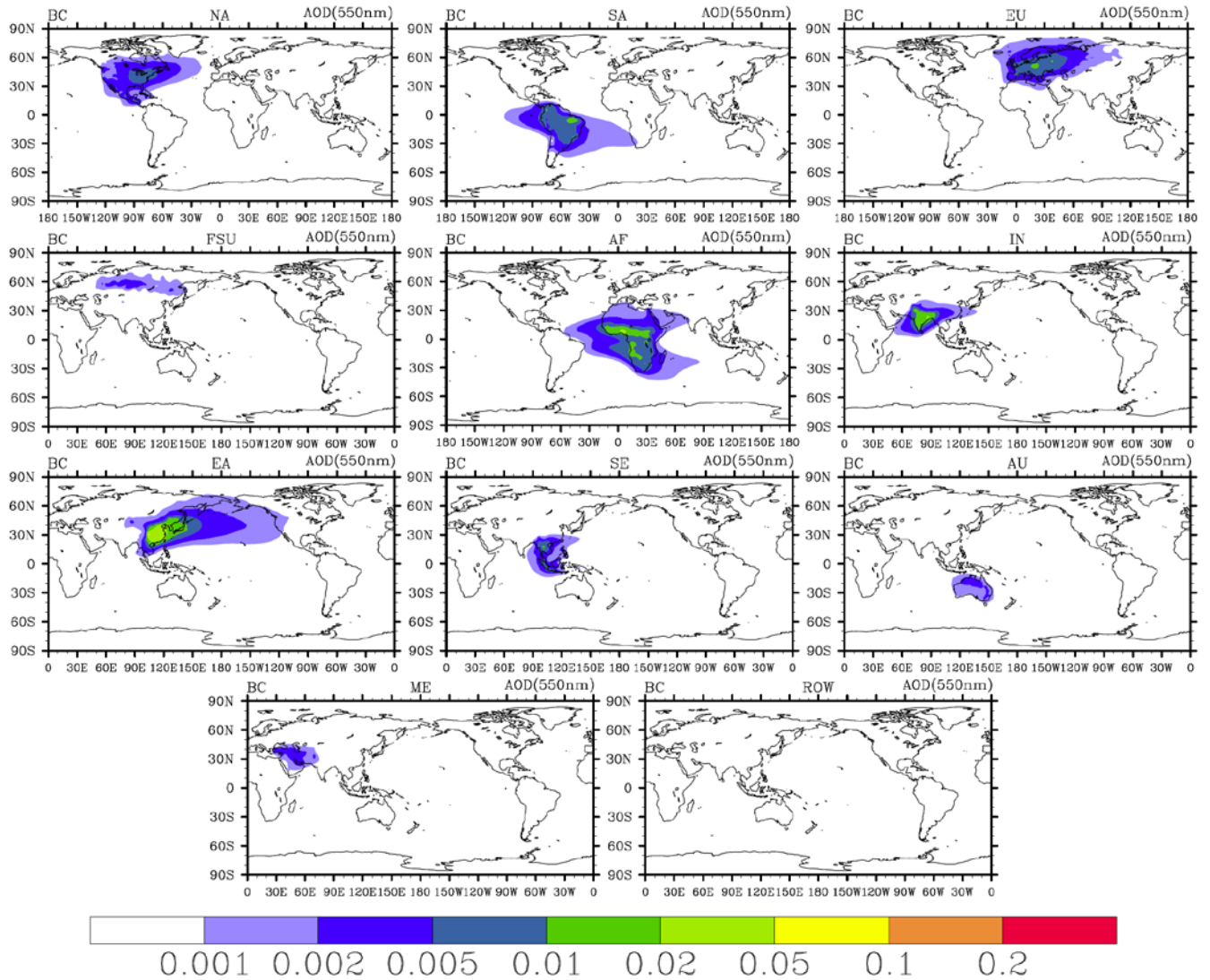


Figure A6 Same as Figure A2, but for BC AOD

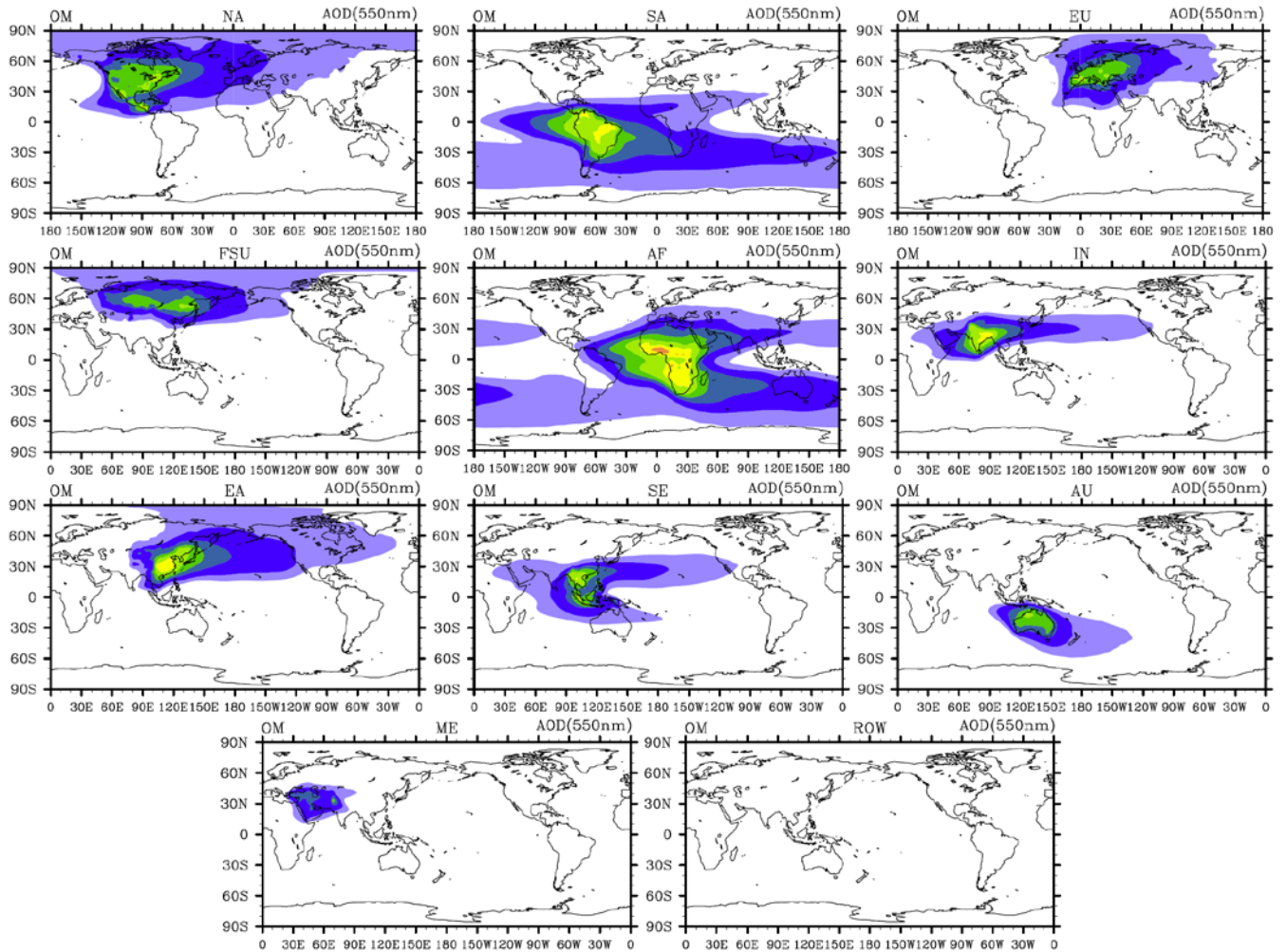


Figure A7 Same as Figure A3, but for OM AOD

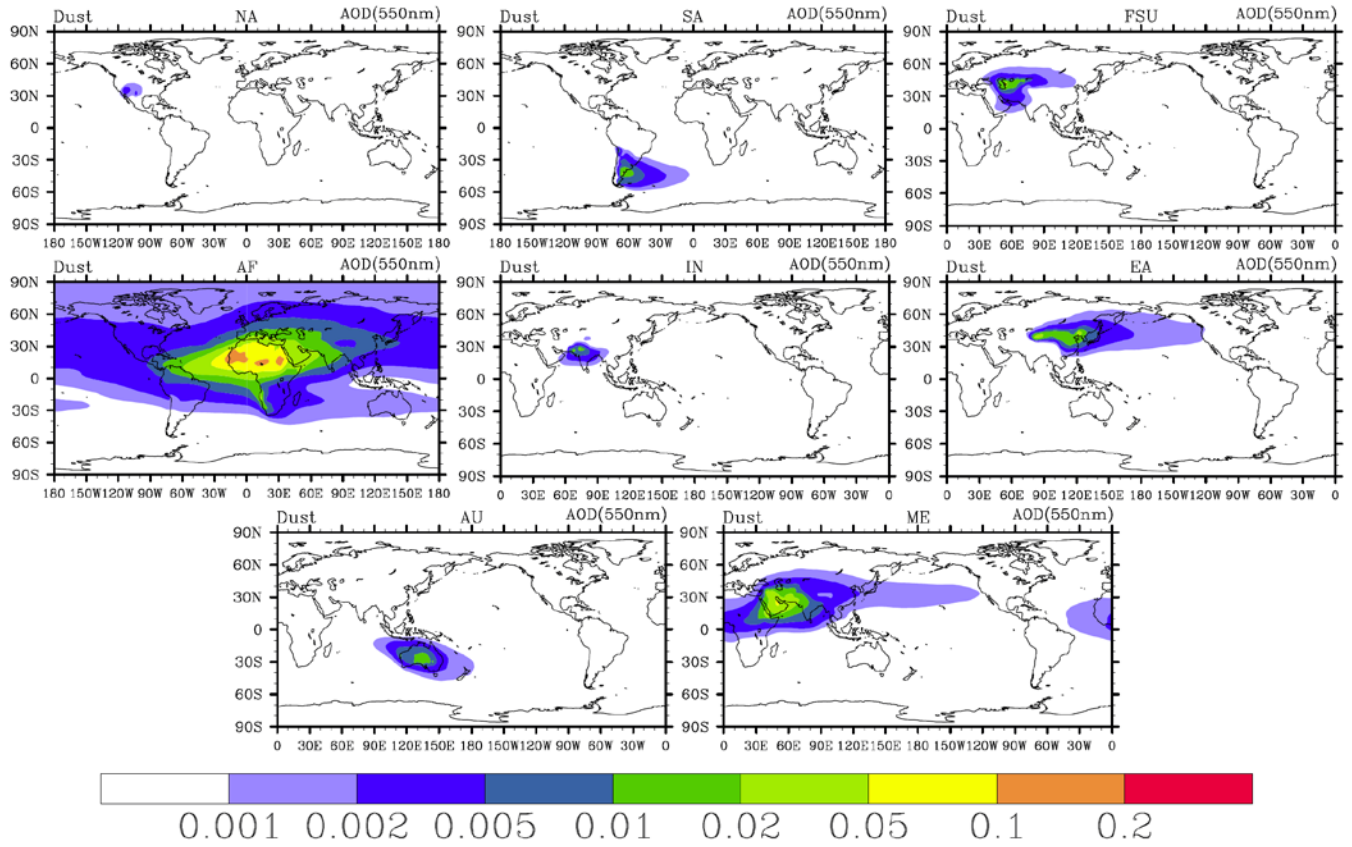


Figure A8 Same as Figure A4, but for dust AOD

Part II Detailed Model evaluation

1. Sulfate

1.1 IMPROVE observations (1997-2003 average)

Figure E1 shows the relative difference between mean annual simulated and observed sulfate concentrations (1997-2003 average) over each IMPROVE observation site (site information is given in Table E1). The annual mean simulated sulfate concentrations generally agree within a factor of 2 with the observations (from Figure 3 in the paper). However, the model underestimates sulfate concentrations in central California and along the US-Mexico border, as well as a few sites over the Eastern US. In contrast, the model overestimates sulfate concentrations over a few sites in western and northeastern US (see Figure E1).

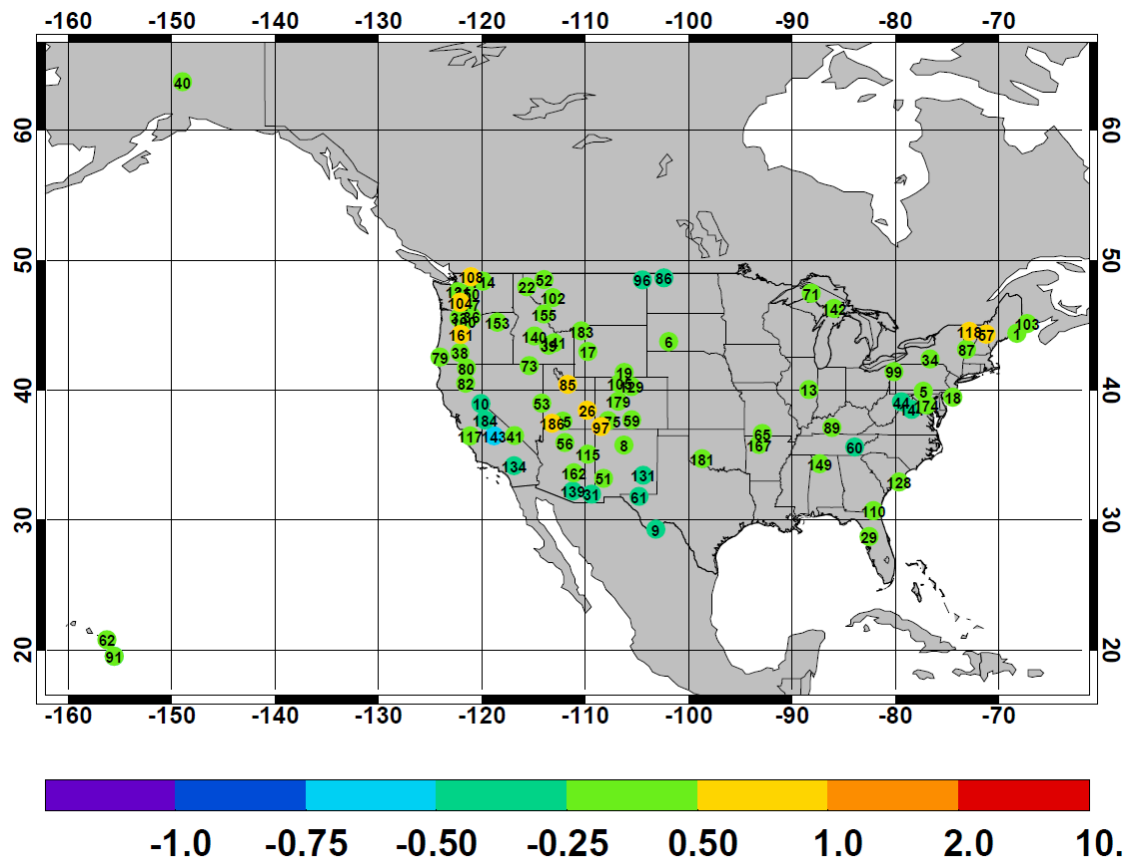
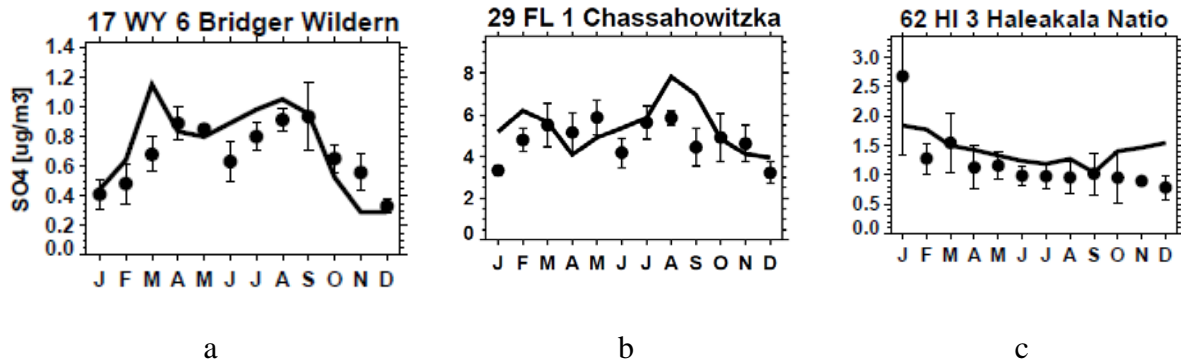


Figure E1 Relative difference (i.e., (model-obs)/obs, shown in color) between the simulated (MOZART-2, 1997-2003 average) and observed IMPROVE annual mean sulfate concentrations (SO_4^{2-} ; $\mu\text{g}\cdot\text{m}^{-3}$; 1997-2003 average). Numbers inside the circles indicate the site index (see Table E1).

The model captures seasonal variability over more than 60% of the IMPROVE sites. See Figure E2 for examples from the ~100 IMPROVE sites we used for sulfate SAC evaluation. Note the change of scale in each figure. The model underestimates summer peak sulfate concentrations over Southwest US (see Figure E2g for an example in central CA). In contrast, the model overestimates spring sulfate concentrations over a few sites in WA and OR (see Figure E2h for an example in WA), overestimates summer sulfate in Northeast US (particularly NH, see Figure E2i), and simulates an opposite seasonal pattern over a few sites in Utah where concentrations are very low (see Figure E2j). These biases may come from the inaccuracy of emission inventories (i.e. seasonal variability, emission height and total emission amount), simplifications of liquid-phase reactions and wet –removal, as well as variability in transport.



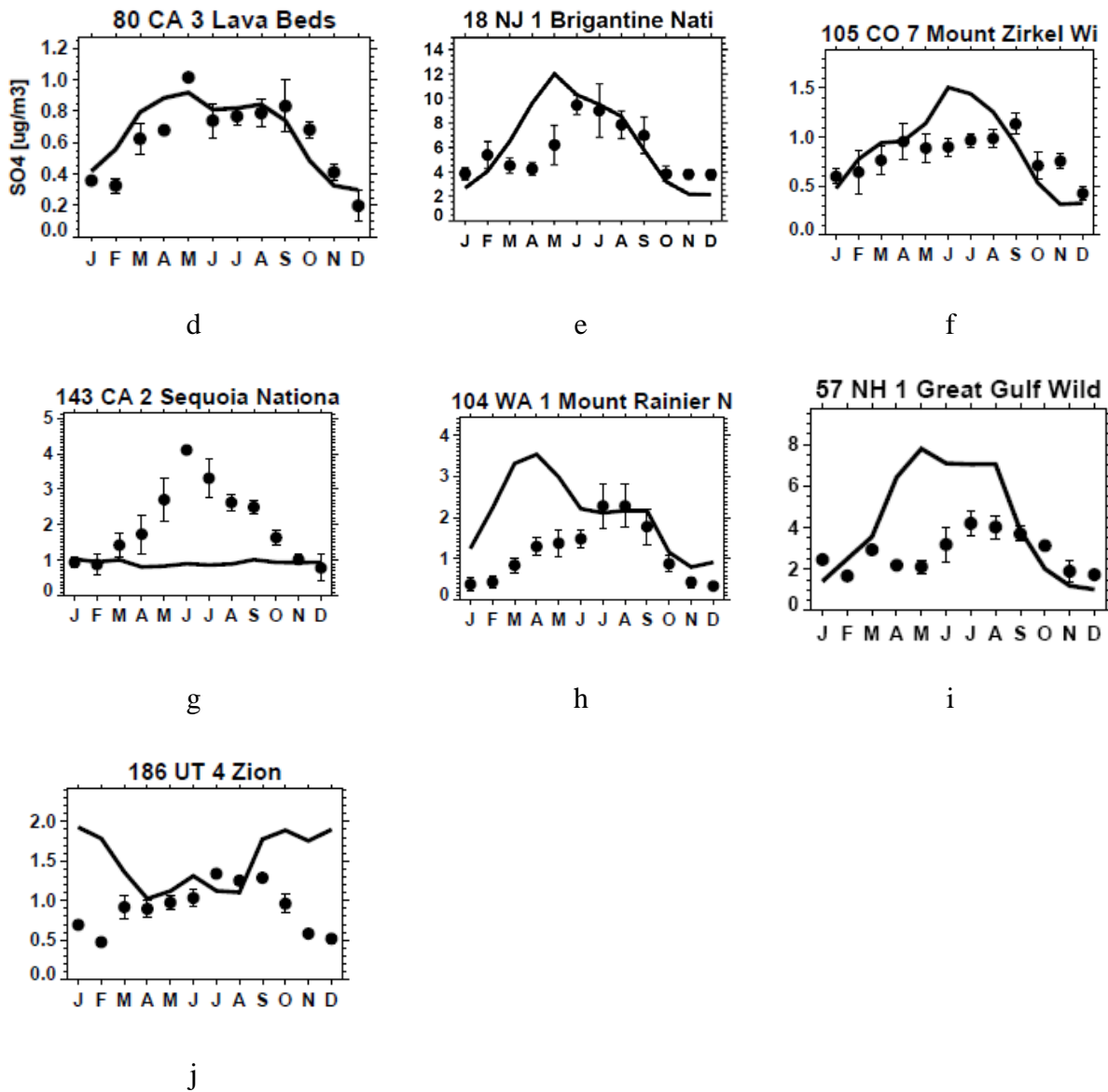


Figure E2 Comparison between simulated (solid line) and observed (dots) monthly SO₄²⁻ (1997-2003 average) over several IMPROVE observation sites (detailed location of each site can be tracked by the site index of both Figure E2 and Table E1).

Table E1 Identifying information for sites in the IMPROVE observation network.

Index	Site	State	Elevation(m)	Latitude	Longitude	Start Date	End Date	Site Name
1	ACAD1	ME	150	44.3771	-68.2612	1988-3-2		Acadia National Park
2	ADPI1	NY	528	42.0911	-77.2098	2001-4-7		Addison Pinnacle
3	AGTI1	CA	507	33.4637	-116.971	2000-11-15		Agua Tibia
4	ARCH1	UT	1722	38.7833	-109.583	1988-3-2	1992-5-1	Arches National Park
5	AREN1	PA	268	39.9231	-77.3078	2001-4-13		Arendtsville
6	BADL1	SD	736	43.7435	-101.941	1988-3-2		Badlands National Park
7	BALD1	AZ	2513	34.0584	-109.441	2000-2-29		Mount Baldy
8	BAND1	NM	1987	35.7797	-106.266	1988-3-2		Bandelier National Monument
9	BIBE1	TX	1075	29.3028	-103.178	1988-3-2		Big Bend National Park
10	BLIS1	CA	2116	38.9756	-120.102	1990-11-17		Bliss State Park (TRPA)
11	BLMO1	MN	476	42.7158	-96.1913			Blue Mounds
12	BOAP1	NM	1383	33.8695	-106.852	2000-4-5		Bosque del Apache
13	BOND1	IL	211	40.0514	-88.3719	2001-3-5		Bondville
14	BOWA1	MN	523.8	47.9464	-91.4961	1991-8-14		Boundary Waters Canoe Area
15	BRCA1	UT	2477	37.6184	-112.174	1988-3-2		Bryce Canyon National Park
16	BRET1	LA	2	29.1186	-89.2065	2000-6-18		Breton
17	BRID1	WY	2607	42.9749	-109.757	1988-3-2		Bridger Wilderness
18	BRIG1	NJ	5	39.465	-74.4492	1991-9-18		Brigantine National Wildlife Refuge
19	BRLA1	WY	3196	41.3662	-106.242	1993-7-31		Brooklyn Lake
20	BRMA1	ME	242	44.1074	-70.7293	2001-3-20		Bridgton
21	CABA1	ME	15	43.8325	-70.0643	2001-3-20		Casco Bay
22	CABI1	MT	1434	47.955	-115.671	2000-7-24		Cabinet Mountains
23	CACO1	MA	41	41.9758	-70.0247	2001-4-1		Cape Cod
24	CACR1	AR	690	34.4543	-94.1429	2000-6-22		Caney Creek
25	CADI1	KY	188	36.7854	-87.8504	2001-3-4		Cadiz
26	CANY1	UT	1799	38.4587	-109.821	1988-3-2		Canyonlands National Park
27	CAPI1	UT	1890	38.3022	-111.293	2000-3-28		Capitol Reef (CAPI1)
28	CEBL1	KS	671	38.7	-99.9			Cedar Bluff
29	CHAS1	FL	2	28.7485	-82.5549	1993-4-3		Chassahowitzka National Wildlife
30	CHER1	OK	335	36.9333	-97.0167			Cherokee Nation
31	CHIR1	AZ	1570	32.0089	-109.389	1988-3-2		Chiricahua National Monument
32	CLPE1	WY	2469	44.3335	-106.957			Cloud Peak
33	COGO1	WA	225	45.5695	-122.212	1996-9-16	1998-5-30	Columbia Gorge
34	COHI1	NY	505	42.4009	-76.6535	2001-4-11		Connecticut Hill
35	COHU1	GA	743	34.7852	-84.6263	2000-5-24		Cohutta
36	CORI1	WA	201.1	45.6678	-121.023	1993-6-26		Columbia River Gorge

37	CRES1	NE	1204	41.7627	-102.434			Crescent Lake
38	CRLA1	OR	1963	42.8962	-122.136	1988-3-2		Crater Lake National Park
39	CRMO1	ID	1817	43.4606	-113.555	1992-5-13		Craters of the Moon NM(US DOE)
40	DENA1	AK	658.2	63.7233	-148.968	1988-3-2		Denali National Park
41	DEVA1	CA	124.9	36.5088	-116.847	1993-10-20		Death Valley Monument
42	DOLA1	CA	914	35.6987	-118.202	1994-8-10		Dome Lands Wilderness
43	DOME1	CA	925	35.7279	-118.138	2000-2-1		Dome Lands Wilderness
44	DOSO1	WV	1158	39.107	-79.4263	1991-9-25		Dolly Sods /Otter Creek Wilderness
45	ELDO1	MO	293	37.69	-94.035			El Dorado Springs
46	ELLI1	OK	701	36.0852	-99.9349			Ellis
47	EVER1	FL	3	25.391	-80.6807	1988-9-28	1999-8-21	Everglades National Park
48	FLAT1	MT	1576	47.7734	-114.269			Flathead
49	FOPE1	MT	885	48.308	-105.102			Fort Peck
50	GAMO1	MT	2392	46.8263	-111.711	2000-7-25		Gates of the Mountains
51	GICL1	NM	1776	33.2204	-108.235	1994-4-6		Gila Wilderness
52	GLAC1	MT	979	48.5105	-113.997	1988-3-2		Glacier National Park
53	GRBA1	NV	2068	39.0052	-114.216	1992-5-27		Great Basin National Park
54	GRCA1HS	AZ	2164	36.0658	-112.154	1989-8-2	1996-6-15	Hopi Point #2 (High Sensitivity)
55	GRCA1	AZ	2164	36.0667	-112.15	1988-3-2	1998-8-29	Hopi Point #1
56	GRCA2	AZ	2267	35.9731	-111.984	1997-9-24		Hance Camp at Grand Canyon NP
57	GRGU1	NH	445	44.3082	-71.2177	1995-6-10		Great Gulf Wilderness
58	GRR11	WI	380	43.9374	-91.4052			Great River Bluffs
59	GRSA1	CO	2504	37.7249	-105.519	1988-5-4		Great Sand Dunes National Monument
60	GRSM1	TN	815	35.6334	-83.9417	1988-3-2		Great Smoky Mountains National Park
61	GUM01	TX	1674	31.833	-104.809	1988-3-2		Guadalupe Mountains National Park
62	HALE1	HI	1157.9	20.8086	-156.282	1991-2-16		Haleakala National Park
63	HAVO1	HI	1204	19.4309	-155.258	1988-3-23		Hawaii Volcanoes National Park
64	HECA1	OR	625	44.9932	-116.84	2000-8-1		Hells Canyon
65	HEGL1	MO	425	36.6713	-92.8781	2001-3-2		Hercules-Glades
66	HILL1	AZ	1510	34.4289	-112.963	2001-4-16		Hillside
67	HOOV1	CA	2566	38.0887	-119.176	2001-7-1		Hoover
68	IKBA1	AZ	1303	34.3403	-111.682	2000-4-2		Ike's Backbone
69	INGA1	AZ	1166	36.0776	-112.129	1989-10-4		Indian Gardens
70	INGA1HS	AZ	1166	36.0776	-112.129	1989-10-4	1992-5-26	Indian Gardens 2 (High Sensitivity)
71	ISLE1	MI	185.8	47.4607	-88.1458	1999-11-16		Isle Royale National Park (New)

72	ISRO1	MI	213	47.9167	-89.15	1988-6-1	1991-7-27	Isle Royale National Park
73	JARB1	NV	1882	41.8926	-115.426	1988-3-2		Jarbidge Wilderness
74	JARI1	VA	299	37.6266	-79.5125	2000-12-5		James River Face
75	JEFF1	VA	219	37.6167	-79.4833	1994-9-3		Jefferson/James River Face Wilderness
76	JOSH1	CA	1228	34.0695	-116.389	2000-2-22		Joshua Tree
77	JOTR1	CA	1228	34.0695	-116.389	1991-9-4	1992-7-8	Joshua Tree National Monument
78	KAIS1	CA	2573	37.2181	-119.156	2000-1-26		Kaiser
79	KALM1	OR	90	42.5519	-124.059	2000-3-7		Kalmiopsis
80	LABE1	CA	1469	41.7117	-121.507	2000-3-25		Lava Beds
81	LASU1	IA	210	40.6883	-91.9883			Lake Sugema
82	LAVO1	CA	1755.2	40.5403	-121.578	1988-3-2		Lassen Volcanic National Park
83	LIGO1	NC	986	35.9722	-81.9331	2000-3-29		Linville Gorge
84	LIVO1	IN	298	38.5347	-86.2608	2001-3-6		Livonia
85	LOPE1	UT	1768	40.4449	-111.708	1993-12-1	2001-8-29	Lone Peak Wilderness
86	LOST1	ND	692	48.642	-102.402	1999-12-15		Lostwood
87	LYBR1	VT	1006	43.1481	-73.1267	1991-9-21		Lye Brook Wilderness
88	LYND1	WA	28	48.9533	-122.559	1996-10-16	1997-8-30	Lynden
89	MACA1	KY	248	37.1315	-86.1477	1991-9-4		Mammoth Cave National Park
90	MALO1	HI	3400	19.5389	-155.578	1992-12-2		Mauna Loa National Observatory (MALO1)
91	MALO2	HI	3400	19.5389	-155.578	1992-12-2		Mauna Loa National Observatory (MALO2)
92	MALO3	HI	3400	19.5389	-155.578	1996-4-3	1996-5-18	Mauna Loa National Observatory (MALO3)
93	MALO4	HI	3400	19.5389	-155.578	1996-4-3	1996-5-18	Mauna Loa National Observatory (MALO4)
94	MAVI1	MA	2	41.3333	-70.8161			Martha's Vineyard
95	MEAD1	AZ	910	36.0194	-114.068	1991-9-4	1992-9-3	Meadview
96	MELA1	MT	605	48.4872	-104.476	1999-12-15		Medicine Lake
97	MEVE1	CO	2177	37.1984	-108.491	1988-3-5		Mesa Verde National Park
98	MING1	MO	112	36.9717	-90.1432	2000-5-24		Mingo
99	MKGO1	PA	387	41.4269	-80.1445	2001-4-17		M. K. Goddard
100	MOHO1	OR	1340.8	45.2927	-121.769	2000-3-7		Mount Hood
101	MOMO1	CT	532	41.8214	-73.2973	2001-9-28		Mohawk Mt.
102	MONT1	MT	1293	47.1222	-113.154	2000-3-28		Monture
103	MOOS1	ME	94	45.1259	-67.2661	1994-12-7		Moosehorn NWR
104	MORA1	WA	427	46.7579	-122.123	1988-3-2		Mount Rainier National Park
105	MOZI1	CO	3243	40.5383	-106.677	1994-7-30		Mount Zirkel Wilderness
106	NEBR1	NE	875	41.8887	-100.339			Nebraska National Forest
107	NOAB1	WY	2480	44.7448	-109.382	2000-1-25		North Absaroka
108	NOCA1	WA	576	48.7316	-121.065	2000-3-1		North Cascades

109	NOCH1	MT	1332	45.6493	-106.557			Northern Cheyenne
110	OKEF1	GA	49	30.7404	-82.1284	1991-9-28		Okefenokee National Wildlife Refuge
111	OLTO1	ME	65	44.9335	-68.6457	2001-7-7		Old Town
112	OLYM1	WA	600	48.0065	-122.973	2001-7-11		Olympic
113	ORPI1	AZ	505	31.9506	-112.802			Organ Pipe
114	PASA1	WA	1634	48.3877	-119.928	2000-11-15		Pasayten
115	PEFO1	AZ	1767.4	35.0781	-109.768	1988-3-2		Petrified Forest National Park
116	PHOE1	AZ	338	33.5038	-112.096	2001-4-25		Phoenix
117	PINN1	CA	316.9	36.485	-121.156	1988-3-2		Pinnacles National Monument
118	PMRF1	VT	403	44.5286	-72.8687	1993-12-22	1995-5-31	Proctor Maple R. F.
119	PORE1	CA	85	38.1199	-122.912	1988-3-2		Point Reyes National Seashore
120	PRIS1	ME	163	46.6963	-68.0335	2001-3-20		Presque Isle
121	PUSO1	WA	80	47.5696	-122.312	1996-3-23		Puget Sound
122	QUCI1	OH	376	39.9429	-81.3378	2001-5-2		Quaker City
123	QURE1	MA	315	42.2988	-72.335	2001-3-20		Quabbin Summit
124	QUVA1	AZ	658	33.2939	-111.286	2001-4-30		Queen Valley
125	RAFA1	CA	953	34.7339	-120.007	2000-2-2		San Rafael
126	REDW1	CA	245	41.56	-124.086	1988-3-2		Redwood National Park
127	RMHQ1	CO	2408	40.25	-105.55	1988-3-2	1990-9-15	Rocky Mountain National Park (Headquarters)
128	ROMA1	SC	3	32.9415	-79.6572	1994-9-3		Cape Romain National Wildlife Refuge
129	ROMO1	CO	2755	40.2783	-105.546	1990-9-19		Rocky Mountain National Park
130	SAAN1	NM	1326	32.6869	-106.484	1997-10-15	2000-8-30	San Andres
131	SACR1	NM	1077	33.4597	-104.404	2000-4-6		Salt Creek
132	SAFO1	NE	293	39.9789	-95.5677			Sac and Fox
133	SAGA1	CA	1791	34.2969	-118.028	2000-12-15		San Gabriel
134	SAGO1	CA	1705	34.1924	-116.901	1988-3-2		San Geronio Wilderness
135	SAGU1	AZ	933	32.1742	-110.737	1988-6-4		Saguaro National Monument
136	SALM1	ID	2788	45.1588	-114.026	1993-12-4	2000-8-31	Salmon National Forest
137	SAMA1	FL	2	30.0926	-84.1614	2000-6-13		St. Marks
138	SAPE1	NM	2918.9	36.014	-106.845	2000-8-15		San Pedro Parks
139	SAWE1	AZ	718	32.2486	-111.218	2001-4-19		Saguaro West
140	SAWT1	ID	1980	44.1706	-114.928	1994-1-26		Sawtooth National Forest
141	SCOV1	ID	1500	43.65	-113.033	1992-5-13	1997-5-24	Scoville
142	SENE1	MI	216.3	46.2881	-85.9461	1999-11-16		Seney
143	SEQU1	CA	535	36.4894	-118.829	1992-3-4		Sequoia National Park
144	SHEN1	VA	1098	38.5229	-78.4347	1988-3-2		Shenandoah National Park
145	SHRO1	NC	1621	35.3937	-82.7743	1994-7-20		Shining Rock Wilderness
146	SIAN1	AZ	1595	34.0909	-110.942	2000-2-10		Sierra Ancha

147	SIKE1	LA	45	32.058	-92.4334	2001-3-22		Sikes
148	SIME1	AK	57	55.3255	-160.506	2001-9-10		Simeonof
149	SIPS1	AL	279	34.3433	-87.3388	1992-3-7		Sipsey Wilderness
150	SNPA1	WA	1160	47.4204	-121.428	1993-7-3		Snoqualamie Pass, Snoqualamie N.F
151	SOLA1	CA	1900	38.9333	-119.967	1989-3-25	1998-5-30	South Lake Tahoe
152	SPOK1	WA	548	47.9045	-117.861	2001-7-11		Spokane Res.
153	STAR1	OR	1258	45.2249	-118.513	2000-3-7		Starkey
154	STPE1	CO	3220	40.445	-106.74	1993-12-1	1994-7-27	Mount Zirkel Wilderness (Storm Peak)
155	SULA1	MT	1903	45.8599	-114	1994-8-10		Sula (Selway Bitterroot Wilderness)
156	SWAN1	NC	2	35.451	-76.2074	2000-6-8		Swanquarter
157	SYCA1	AZ	2039.6	35.1406	-111.969	1991-9-11	1992-7-8	Sycamore Canyon
158	TALL1	KS	387	38.3	-96.6			Tallgrass
159	THBA1	WY	1193	44.6634	-105.287			Thunder Basin
160	THRO1	ND	853	46.8948	-103.378	1999-12-15		Theodore Roosevelt
161	THSI1	OR	885	44.291	-122.043	1993-7-24		Three Sisters Wilderness
162	TONT1	AZ	786	33.6494	-111.109	1988-4-23		Tonto National Monument
163	TRCR1	AK	155	62.3153	-150.316	2001-9-10		Trapper Creek
164	TRIN1	CA	1007	40.7865	-122.805	2000-7-19		Trinity
165	TUXE1	AK	15	59.9925	-152.666	2001-12-18		Tuxedni
166	ULBE1	MT	893	47.5823	-108.72	2000-1-25		UL Bend
167	UPBU1	AR	723	35.8259	-93.2029	1991-12-18		Upper Buffalo Wilderness
168	VIIS1	VI	64	18.3384	-64.795	1990-10-13		Virgin Islands National Park
169	VILA1	IA	426	40.9712	-95.0439			Viking Lake
170	VOYA1	MN	347	48.5833	-93.1667	1988-3-2	1996-9-28	Voyageurs National Park 1
171	VOYA2	MN	429	48.4126	-92.8286	1999-11-16		Voyageurs National Park 2
172	WALT1	NE		42.1	-96.4			Omaha Tribe
173	WARI1	NV	1255	38.9519	-118.815			Walker River
174	WASH1	DC	16	38.8761	-77.0343	1988-3-1		Washington D.C.
175	WEMI1	CO	2765	37.6594	-107.8	1988-3-2		Weminuche Wilderness
176	WHIT1	NM	2050	33.4698	-105.523	2002-1-15		White Mountain
177	WHPA1	WA	1830	46.6244	-121.388	2000-2-15		White Pass
178	WHPE1	NM	3372	36.5855	-105.451	2000-8-15		Wheeler Peak
179	WHRI1	CO	3418	39.1517	-106.819	1993-7-17		White River National Forest
180	WICA1	SD	1300	43.5577	-103.484	1999-12-15		Wind Cave
181	WIMO1	OK	518	34.7315	-98.7155	2001-3-1		Wichita Mountains
182	YELL1	WY	2361	44.5625	-110.373	1988-3-9	1996-7-1	Yellowstone National Park 1
183	YELL2	WY	2425	44.5653	-110.4	1996-7-1		Yellowstone National Park 2
184	YOSE1	CA	1615	37.7125	-119.704	1988-3-9		Yosemite National Park

185	ZICA1	UT	1236	37.1952	-113.14	2003-2-2		Zion
186	ZION1	UT	1545	37.4591	-113.224	2000-3-21		Zion

1.2 EMEP observations (1997-2003 average):

We also evaluate our simulated sulfate concentrations with EMEP observations. As shown in Figure E3, the simulated annual mean sulfate concentrations agree within a factor of 2 with more than 85% of the EMEP observations. However, the model tends to systematically overestimate summer sulfate concentrations over more than 50% of observation sites, particularly over Iceland, Ireland, France, Switzerland, Norway, Sweden, Latvia, and Estonia (see a few typical sites in Figure E4). Possible reasons include the bias from the wet deposition rates (*Horowitz 2006*) as well as that the emissions inventory we used (IIASA RAINS CLE2000) may overestimate the SO₂ emissions in Europe for the year 2000, particularly in summer.

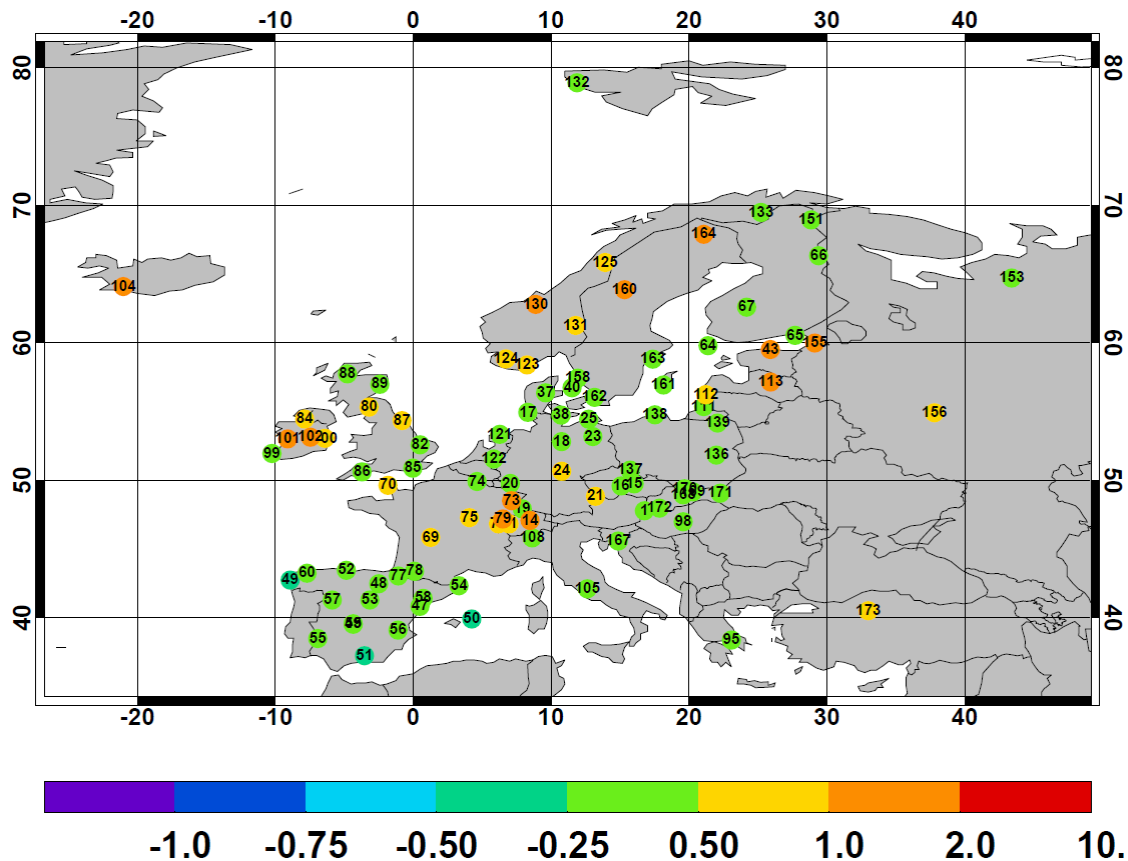


Figure E3 Same as Figure E1, but for EMEP sulfate observations (site information is given in Table E2).

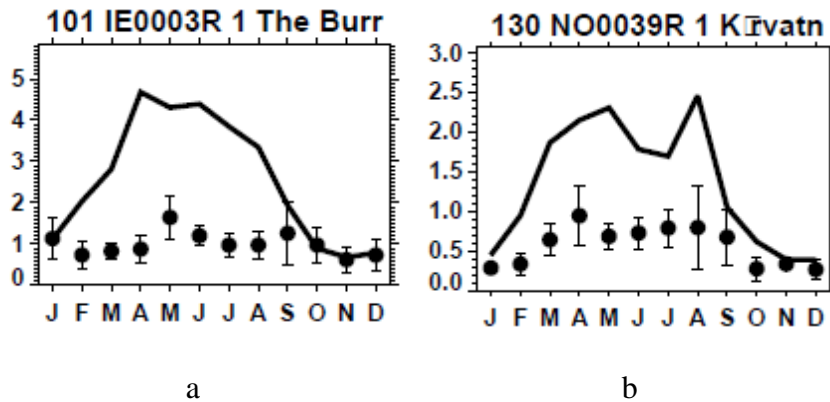


Figure E4 Comparison between simulated and observed monthly SO_4^{2-} concentrations (1997-2003 average) over a few EMEP observation sites (site info is given in Table E2).

Table E2 Identifying information for EMEP observation sites

Index	Code	Station name	Lat	Lon	Alt
1	AT0002R	Illmitz	47.77	16.77	117
2	AT0003R	Achenkirch	47.55	11.72	960
3	AT0004R	St. Koloman	47.65	13.2	851
4	AT0005R	Vorhegg	46.68	12.97	1020
5	BA0006R	Ivan Sedlo	43.77	18.03	970
6	BE0001R	Offagne	49.88	5.2	430
7	BE0032R	Eupen	50.63	6	295
8	BE0035R	Vezin	50.5	4.99	160
9	BY0004R	Vysokoe	52.33	23.43	163
10	CH0001G	Jungfrauoch	46.55	7.98	3573
11	CH0002R	Payerne	46.82	6.95	510
12	CH0003R	T 鋁 ikon	47.48	8.9	540
13	CH0004R	Chaumont	47.05	6.98	1130
14	CH0005R	Rigi	47.07	8.47	1030
15	CZ0001R	Svratouch	49.73	16.03	737
16	CZ0003R	Kosetice	49.58	15.08	534
17	DE0001R	Westerland	54.93	8.31	12
18	DE0002R	Langenbr 黠 ge	52.8	10.76	74
19	DE0003R	Schauinsland	47.91	7.91	1205
20	DE0004R	Deuselbach	49.76	7.05	480
21	DE0005R	Brotjacklriegel	48.82	13.22	1016
22	DE0006R	Arkona	54.68	13.43	42
23	DE0007R	Neuglobsow	53.17	13.03	62
24	DE0008R	Schm 黠 ke	50.65	10.77	937
25	DE0009R	Zingst	54.43	12.73	1
26	DE0011R	Hohenwestedt	54.1	9.67	75
27	DE0012R	Bassum	52.85	8.7	52
28	DE0013R	Rodenberg	52.32	9.37	148
29	DE0014R	Meinerzhagen	51.12	7.63	510
30	DE0015R	Usingen	50.33	8.53	485
31	DE0016R	Bad Kreuznach	49.83	7.87	230
32	DE0017R	Ansbach	49.3	10.57	481
33	DE0018R	Rottenburg	48.48	8.93	427
34	DE0019R	Starnberg	48.02	11.35	729
35	DE0020R	Hof	50.32	11.88	568
36	DK0001R	F 錄 鴈 rne	61.3	-7.07	210
37	DK0003R	Tange	56.35	9.6	13

38	DK0005R	Keldsnor	54.73	10.73	10
39	DK0007R	F 鏢鴈 rne-Akraberg	61.4	-6.67	90
40	DK0008R	Anholt	56.72	11.52	40
41	DK0022R	Sepstrup Sande	55.08	9.6	60
42	EE0002R	Syrve	57.95	22.1	2
43	EE0009R	Lahemaa	59.5	25.9	32
44	EE0011R	Vilsandy	58.38	21.82	6
45	ES0001R	San Pablo de los Montes	39.55	-4.35	917
46	ES0002R	La Cartuja	37.2	-3.6	720
47	ES0003R	Roquetas	40.82	0.49	44
48	ES0004R	Logro 駟	42.46	-2.5	445
49	ES0005R	Noya	42.73	-8.92	683
50	ES0006R	Mah 髒	39.9	4.25	0
51	ES0007R	V 韓 nar	37.23	-3.53	1265
52	ES0008R	Niembro	43.44	-4.85	134
53	ES0009R	Campisabalos	41.28	-3.14	1360
54	ES0010R	Cabo de Creus	42.32	3.32	23
55	ES0011R	Barcarrola	38.48	-6.92	393
56	ES0012R	Zarra	39.09	-1.1	885
57	ES0013R	Penausende	41.28	-5.87	985
58	ES0014R	Els Torms	41.4	0.72	470
59	ES0015R	Risco Llamo	39.52	-4.35	1241
60	ES0016R	O Savi 駟 o	43.23	-7.7	506
61	FI0004R	膝 tari	62.53	24.22	162
62	FI0006R	K 鯨 ar	59.92	20.92	10
63	FI0007R	Violahti	60.52	27.68	8
64	FI0009R	Ut?	59.78	21.38	7
65	FI0017R	Violahti II	60.53	27.69	4
66	FI0022R	Oulanka	66.32	29.4	310
67	FI0037R	Ahtari II	62.58	24.18	180
68	FR0001R	Vert-le-Petit	48.53	2.37	64
69	FR0003R	La Cruzille	45.83	1.27	497
70	FR0005R	La Hague	49.62	-1.83	133
71	FR0006R	Valduc	47.58	4.87	470
72	FR0007R	Lodeve	43.7	3.33	252
73	FR0008R	Donon	48.5	7.13	775
74	FR0009R	Revin	49.9	4.63	390
75	FR0010R	Morvan	47.27	4.08	620
76	FR0011R	Bonnevaux	46.82	6.18	836
77	FR0012R	Iraty	43.03	-1.08	1300

78	FR0013R	Peyrusse Vieille	43.37	0.1	236
79	FR0014R	Montandon	47.18	6.5	746
80	GB0002R	Eskdalemuir	55.31	-3.2	243
81	GB0003R	Goonhilly	50.05	-5.18	108
82	GB0004R	Stoke Ferry	52.57	0.5	15
83	GB0005R	Ludlow	52.37	-2.63	190
84	GB0006R	Lough Navar	54.44	-7.87	126
85	GB0007R	Barcombe Mills	50.87	-0.03	8
86	GB0013R	Yarner Wood	50.6	-3.71	119
87	GB0014R	High Muffles	54.33	-0.81	267
88	GB0015R	Strath Vaich Dam	57.73	-4.77	270
89	GB0016R	Glen Dye	56.97	-2.42	85
90	GB0036R	Harwell	51.57	-1.32	137
91	GB0037R	Ladybower Res.	53.4	-1.75	420
92	GB0038R	Lullington Heath	50.79	0.18	120
93	GB0043R	Narberth	51.23	-4.7	160
94	GB0045R	Wicken Fen	52.3	-0.29	5
95	GR0001R	Aliartos	38.37	23.08	110
96	HR0002R	Puntijarka	45.9	15.97	988
97	HR0004R	Zavizan	44.82	14.98	1594
98	HU0002R	K-puszta	46.97	19.58	125
99	IE0001R	Valentina Observatory	51.94	-10.24	11
100	IE0002R	Turlough Hill	53.04	-6.4	420
101	IE0003R	The Burren	53	-9.1	90
102	IE0004R	Ridge of Capard	53.12	-7.45	340
103	IS0001R	Rjupnahed	64.08	-21.85	120
104	IS0002R	Irafoss	64.08	-21.02	66
105	IT0001R	Montelibretti	42.1	12.63	48
106	IT0002R	Stelvio	46.35	10.38	1415
107	IT0003R	Vallombrosa	3.73	11.55	1000
108	IT0004R	Ispra	45.8	8.63	209
109	IT0005R	Arabba	46.52	11.88	2030
110	LT0003R	Nida	55.35	21.07	17
111	LT0015R	Preila	55.35	21.07	5
112	LV0010R	Rucava	56.22	21.22	5
113	LV0016R	Zoseni	57.13	25.92	183
114	MK0007R	Lazaropole	41.32	20.42	1332
115	MD0012R	Leovo	46.5	28.27	156
116	NL0002R	Witteveen	52.82	6.67	18
117	NL0005R	Rekken	52.1	6.72	25

118	NL0006R	Appelscha	52.95	6.3	10
119	NL0007R	Eibergen	52.08	6.57	20
120	NL0008R	Bilthoven	52.12	5.2	5
121	NL0009R	Kollumerwaard	53.33	6.28	1
122	NL0010R	Vredepeel	51.54	5.85	28
123	N00001R	Birkenes	58.38	8.25	190
124	N00008R	Skre 鋼 alen	58.82	6.72	475
125	N00015R	Tustervatn	65.83	13.92	439
126	N00030R	Jergul	69.4	24.6	255
127	N00035R	Narbuvoll	62.35	11.47	768
128	N00036R	Hummelfjell	62.45	11.27	1539
129	N00037R	Bj 駝 n 鷺 a	74.52	19.02	20
130	N00039R	K 鏢 vatn	62.78	8.88	210
131	N00041R	Osen	61.25	11.78	440
132	N00042G	Spitsbergen Zeppelinfjell	78.9	11.88	474
133	N00055R	Karasjok	69.47	25.22	333
134	N00099R	Lista	58.1	6.57	13
135	PL0001R	Suwalki	54.13	22.95	184
136	PL0002R	Jarczew	51.82	21.98	180
137	PL0003R	Sniezka	50.73	15.73	1603
138	PL0004R	Leba	54.75	17.53	2
139	PL0005R	Diabla Gora	54.15	22.07	157
140	PT0001R	Braganca	41.82	-6.77	690
141	PT0002R	Faro	37.02	-7.97	8
142	PT0003R	Viana do Castelo	41.7	-8.8	16
143	PT0004R	Monte Velho	38.08	-8.8	43
144	PT0005R	Foia	37.32	-8.9	902
145	R00001R	Rarau	47.45	25.45	1536
146	R00002R	Stina de Vale	46.68	23.53	1111
147	R00003R	Semenic	45.12	25.97	1432
148	R00004R	Paring	45.38	23.47	1585
149	R00005R	Fundata	45.47	25.3	1371
150	R0000R6	Turia	46.12	25.98	1008
151	RU0001R	Janiskoski	68.93	28.85	118
152	RU0008R	Lesogorsky	61	28.97	39
153	RU0013R	Pinega	64.7	43.4	28
154	RU0014R	Pushkinskie Gory	57	28.9	103
155	RU0016R	Shepeljovo	59.97	29.12	4
156	RU0018R	Danki	54.9	37.8	150
157	SE0001R	Eker 鰻	55.9	13.72	140

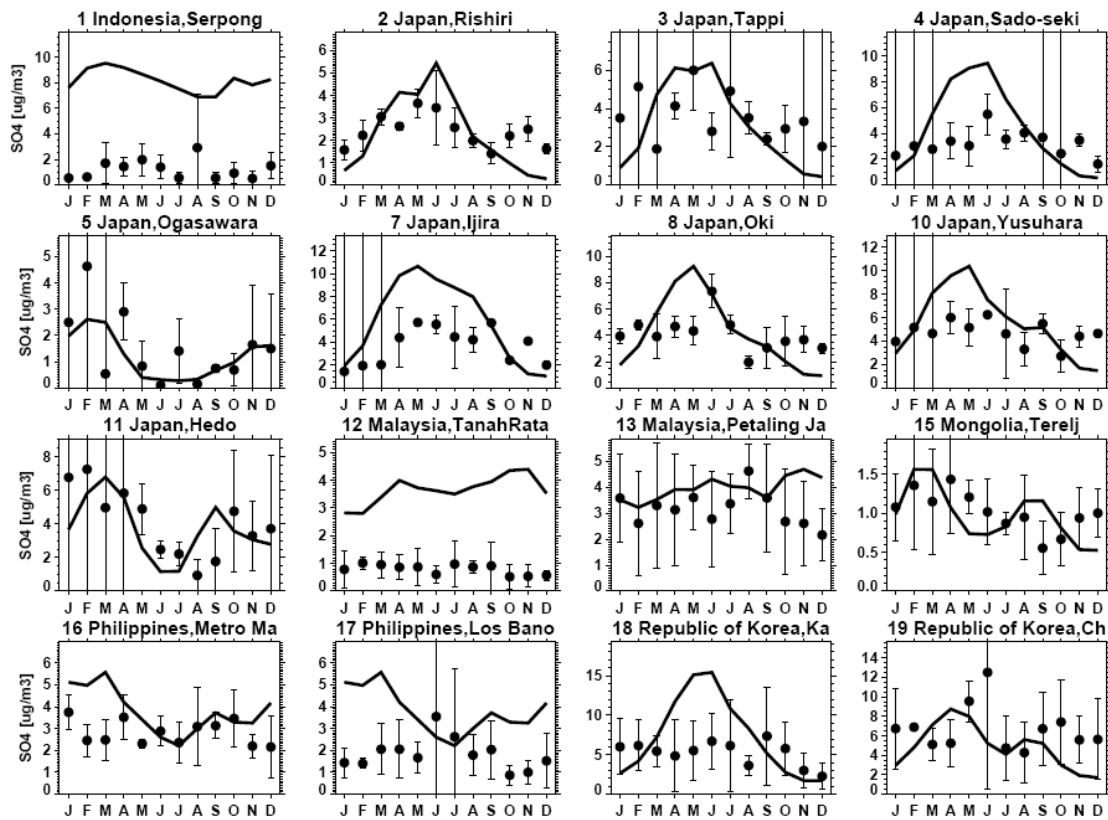
158	SE0002R	R 鯉 vik	57.42	11.93	10
159	SE0003R	Velen	58.78	14.3	127
160	SE0005R	Bredk 鋁 en	63.85	15.33	404
161	SE0008R	Hoburgen	56.92	18.15	58
162	SE0011R	Vavihill	56.02	13.15	175
163	SE0012R	Aspvreten	58.8	17.38	20
164	SE0013R	Estrange	67.88	21.07	475
165	SE0035R	Vindeln	64.25	19.77	225
166	SI0001R	Masun	45.65	14.37	1026
167	SI0008R	Iskrba	45.57	14.87	520
168	SK0002R	Chopok	48.93	19.58	2008
169	SK0004R	Star?Lesn?	49.15	20.28	808
170	SK0005R	Liesek	49.37	19.68	892
171	SK0006R	Starina	49.05	22.27	345
172	SK0007R	Topolniky	47.96	17.86	113
173	TR0001R	Cubuk II	40.5	33	1169
174	UA0005R	Svityaz	51.52	23.88	164
175	UA0006R	Rava-Russkaya	50.25	23.63	249
176	UA0007R	Beregovo	48.25	22.68	112
177	YU0005R	Kamenicki vis	43.4	21.95	813
178	YU0008R	Zabljak	43.15	19.13	1450

1.3 EANET (2000-2004 average, mostly 2003-2004):

Table E3 provides the location and sampling period for each EANET observation site. The simulated annual mean sulfate concentrations generally agree with the EANET observations within a factor of 2 (see Figure 3a in the paper as well as Figure E5). However, the model overestimates early summer (April-June) sulfate concentrations over a few Japanese sites (Figure E5, site# 4,7,8,10), but slightly underestimates sulfate concentrations in winter (DJF, most Japanese sites). This is probably due to the seasonal variation of SO₂ emissions over EA which are not well represented in the model. For example, in China the heating period is Dec.-Mar for North China, and coal is the

primary fuel for heating. Therefore, winter SO₂ emissions are likely larger than in other seasons.

From Figure E5 (site #1 and 12), our model systematically overestimates sulfate concentrations over one location in Indonesia and another one in Malaysia. This is probably due to the constant volcanic emissions included in the model which are likely too large. In addition, the model underestimates sulfate concentrations over several Russian sites (particularly in winter).



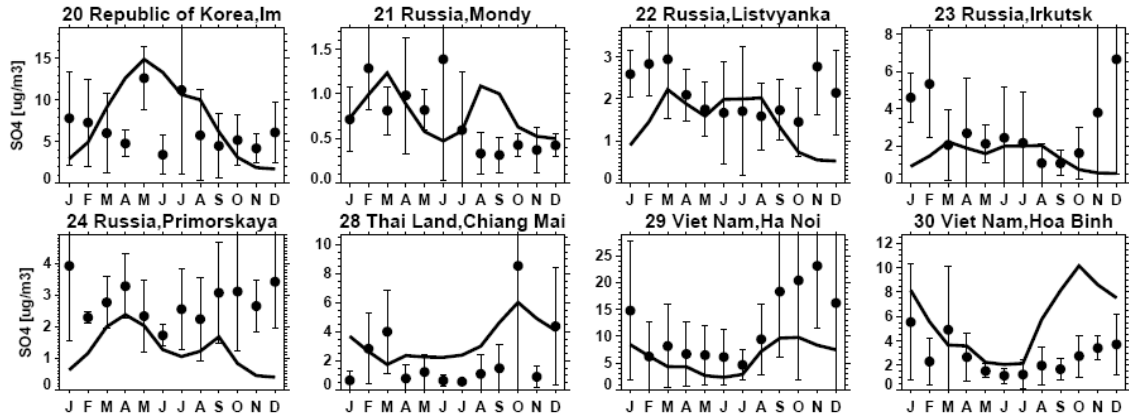


Figure E5 Comparison between simulated and observed monthly SO_4^{2-} concentrations (2000-2004 average) over most EANET observation sites (detailed sampling time and location are given in Table E1).

Table E3 Information for EANET observation sites

Site#	Site name	Location	Start-End time
1	Indonesia,Serpong	-6.25, 106.57	2001-2004
2	Japan,Rishiri	45.12, 141.23	2002-2004
3	Japan,Tappi	41.27, 141.35	2003-2004
4	Japan,Sado-seki	38.25, 138.40	2003-2004
5	Japan,Ogasawara	27.08, 142.22	2003-2004
6	Japan,Happo	36.68, 137.80	2003-2004
7	Japan,Ijira	35.57, 136.70	2003-2004
8	Japan,Oki	36.28, 133.18	2002-2004
9	Japan,Banryu	34.68, 131.80	2003-2004
10	Japan,Yusuhara	33.38, 132.93	2003-2004
11	Japan,Hedo	26.85, 128.25	2003-2004
12	Malaysia,TanahRata	4.47, 101.38	2000-2004
13	Malaysia,Petaling Jaya	3.10, 101.65	2001-2004
14	Mongolia,Ulaanbaatar	47.90, 106.82	2000-2004
15	Mongolia,Terelj	47.98, 107.48	2000-2004
16	Philippines,Metro Manila	14.63, 121.07	2000-2004
17	Philippines,Los Banos	14.18, 121.25	2000-2004
18	Republic of Korea,Kanghwa	37.62, 126.37	2001-2004
19	Republic of Korea,Cheju	33.28, 126.17	2001-2004
20	Republic of Korea,Imsil	35.60, 127.18	2001-2004
21	Russia,Mondy	51.67, 101.00	2000-2004
22	Russia,Listvyanka	51.85, 104.90	2001-2004
23	Russia,Irkutsk	52.23, 104.25	2000-2004
24	Russia,Primorskaya	43.7, 132.12	2001-2004
25	Thai Land,Bangkok	13.77, 100.53	2003-2004
26	Thai Land,Patumthani	14.03, 100.77	2003-2004
27	Thai Land, Khanchanaburi	14.77, 98.58	2004
28	Thai Land,Chiang Mai	18.77,98.93	2001-2004
29	Viet Nam,Ha Noi	21.02,105.85	2000-2004
30	Viet Nam,Hoa Binh	20.82,105.33	2000-2004

1.4 RSMAS observations (1980s-1990s)

Table E4 lists the information for each RSMAS site. As shown in Figure 3a (in the paper) as well as Figure E6, the model tends to systematically overestimate sulfate concentrations over several sites in the southern hemisphere. Possible reasons are that the RSMAS observations include data collected from the early 1980s, when global emissions were quite different than those in 2000. In addition, the model underestimates sulfate concentrations over Bermuda (site#25), probably due to the reduction of SO₂ emissions from the US during the late 1990s (or the bias of trans-Atlantic transport of sulfate by the model).

Both RSMAS and EANET networks have observations over Hedo, Japan, but with different sampling periods. Figures E7a shows the monthly sulfate concentrations averaged over 1991 and 1994 (i.e., RSMAS data). Figure E7b shows the EANET data averaged over 2003 and 2004. In JFM (Jan., Feb. and March), we do see a 20-50% increase in sulfate concentrations from the early 1990s to the early 2000s. However, in other seasons, the sulfate concentrations are actually similar or even decreased from the early 1990s to the early 2000s. This change in sulfate concentrations over Japan likely reflects both increases in SO₂ emissions from mainland EA and decreased local SO₂ emissions from Japan.

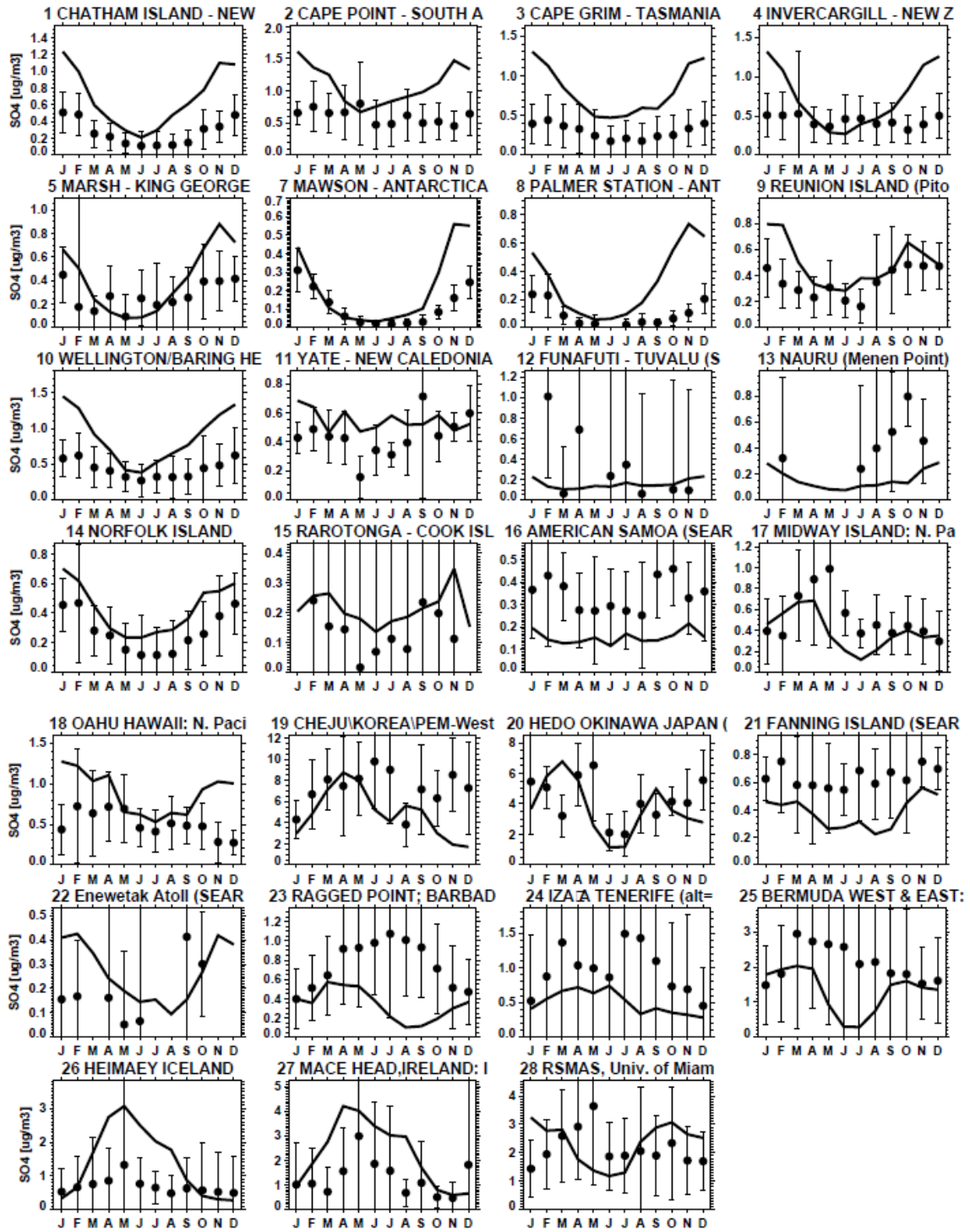
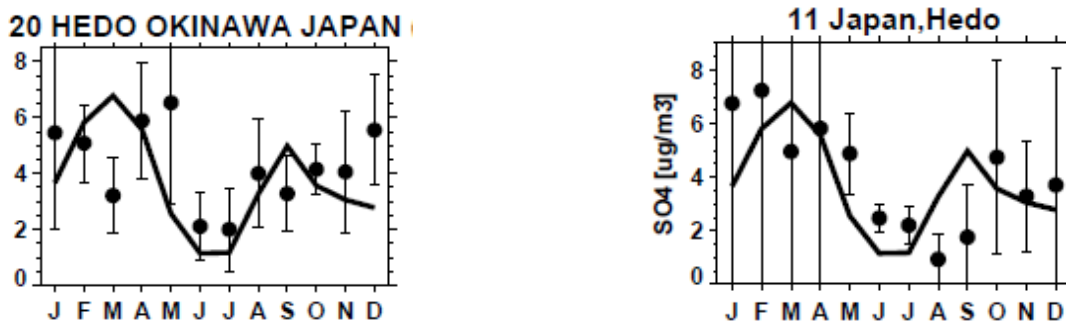


Figure E6 Comparison between simulated and observed RSMAS monthly sulfate concentrations (site info is given in Table E4).

Table E4 Information for RSMAS observation sites

No.	Site Name	Position	Sampling period
1	Chatham Island - New Zealand	43.92°S,176.50°W	16-Sep-1983,11-Oct-1996
2	Cape Point - South Africa	34.35°S,18.48°E	27-Feb-1992,21-Nov-1996
3	Cape Grim - Tasmania	40.68°S,144.68°E	11-Jan-1983,08-Nov-1996
4	Invercargill - New Zealand	46.43°S,168.35°E	22-Apr-1983,15-Nov-1996
5	Marsh - King George Island	62.18°S,58.30°W	27-Mar-1990,25-Sep-1996
6	Marion Island/Prince Edward Island	46.92°S,37.75°E	25-Mar-1992,01-May-1996
7	Mawson - Antarctica	67.60°S,62.50°E	18-Feb-1987,01-Jan-1996
8	Palmer Station - Antarctica	64.77°S,64.05°W	03-Apr-1990,18-Oct-1996
9	REUNION ISLAND	21.17°S,55.83°E	05-Nov-1990,16-Aug-1996
10	Wellington/Baring Head - New Zealand	41.28°S,174.87°E	20-Oct-1987,05-Nov-1996
11	Yate - New Caledonia	22.15°S,167.00°E	23-Aug-1983,23-Oct-1985
12	Funafuti - Tuvalu	8.50°S,179.20°W	08-Apr-1983,31-Jul-1987
13	Nauru	0.53°S,166.95°E	16-Mar-1983,02-Oct-1987
14	Norfolk Island	29.08°S,167.98°E	27-May-1983,21-Feb-1997
15	Rarotonga - Cook Islands	21.25°S,159.75°W	23-Mar-1983,23-Jun-1994
16	American Samoa	14.25°S,170.58°W	19-Mar-1983,03-Jan-1996
17	Midway Island: N. Pacific	28.22°N,177.35°W	18-Jan-1981,02-Jan-1997
18	Oahu Hawaii: N. Pacific	21.33°N,157.70°W	21-Jan-1981,13-Jul-1995
19	Cheju\Korea\Pem-West	33.52°N,126.48°E	10-Sep-1991,27-Oct-1995
20	Hedo Okinawa Japan	26.92°N,128.25°E	01-Sep-1991,18-Mar-1994
21	Fanning Island	3.92°N,159.33°W	02-Apr-1981,14-Aug-1986
22	Enewetak Atoll	11.33°N,162.33°E	27-Feb-1981,10-Jun-1987
23	Ragged Point; Barbados	13.17°N,59.43°W	05-May-1984,01-Jul-1998
24	IZAÑA TENERIFE (Alt=2360 M)	28.30°N,16.50°W	25-Jul-1987,01-Jul-1998
25	Bermuda West & East: Composited Data Set	32.27°N,64.87°W	29-Mar-1989,01-Jan-1998
26	Heimaey Iceland	63.40°N,20.30°W	20-Jul-1991,02-Jan-1998
27	Mace Head, Ireland	53.32°N,9.85°W	11-Aug-1988,15-Aug-1994
28	RSMAS, Univ. Of Miami	25.75°N,80.25°W	02-Jan-1989,07-Aug-1998



a (RSMAS)

b (EANET)

Figure E7 Comparison between simulated and observed monthly SO_4^{2-} concentrations at Hedo, Japan. Observations are (a) RSMAS (1991-1994 average) and (b) EANET (Jan-Apr.: 2004 data; May-Dec.: 2003-2004 average).

2. Black carbon

2.1 IMPROVE observations (1997-2003 average)

As shown in Figure 4a (in the paper), the simulated annual mean BC concentrations agree within a factor of 2 with more than 80% of the observations. However, the model underestimates sulfate concentrations in northern California and the southeast U.S., and overestimates sulfate at a few sites in Washington, California, and New Hampshire (see Figure E8).

The model captures well the seasonal patterns over nearly 60% of IMPROVE sites. Figure E9 (a-f) shows examples of simulated seasonal variability of BC concentrations. However, the model may significantly underestimate BC concentrations over specific months (e.g. May in Figure E9b (NM) and August in Figure E9c (NV)). This is probably due to the bias in seasonal variability in biomass burning BC emissions.

In addition, our model tends to systematically underestimate BC concentrations over northern California (see Figure E9g) and a few sites over the southeastern US (Figure E9h), but overestimate and even have opposite seasonal patterns over a few sites in Washington and New Hampshire (see Figure E9i).

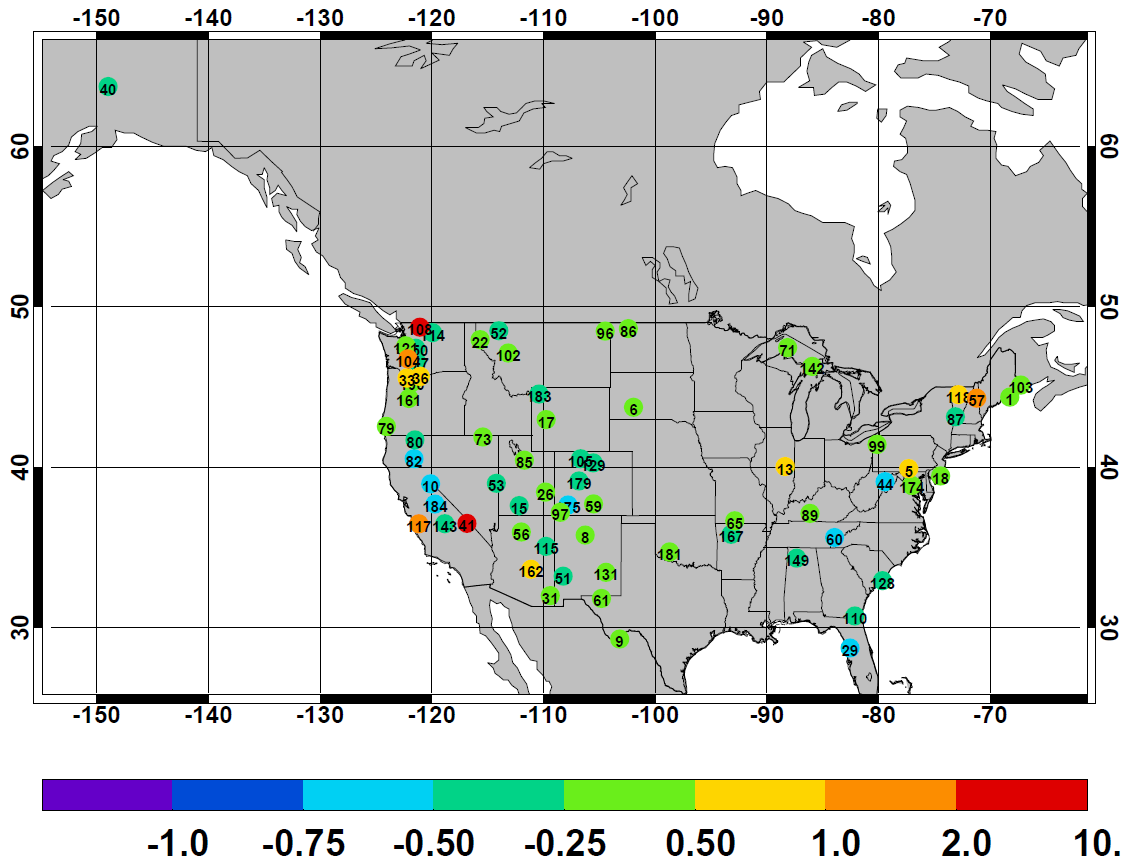


Figure E8 Same as Figure E1, but for black carbon (IMPROVE sites).

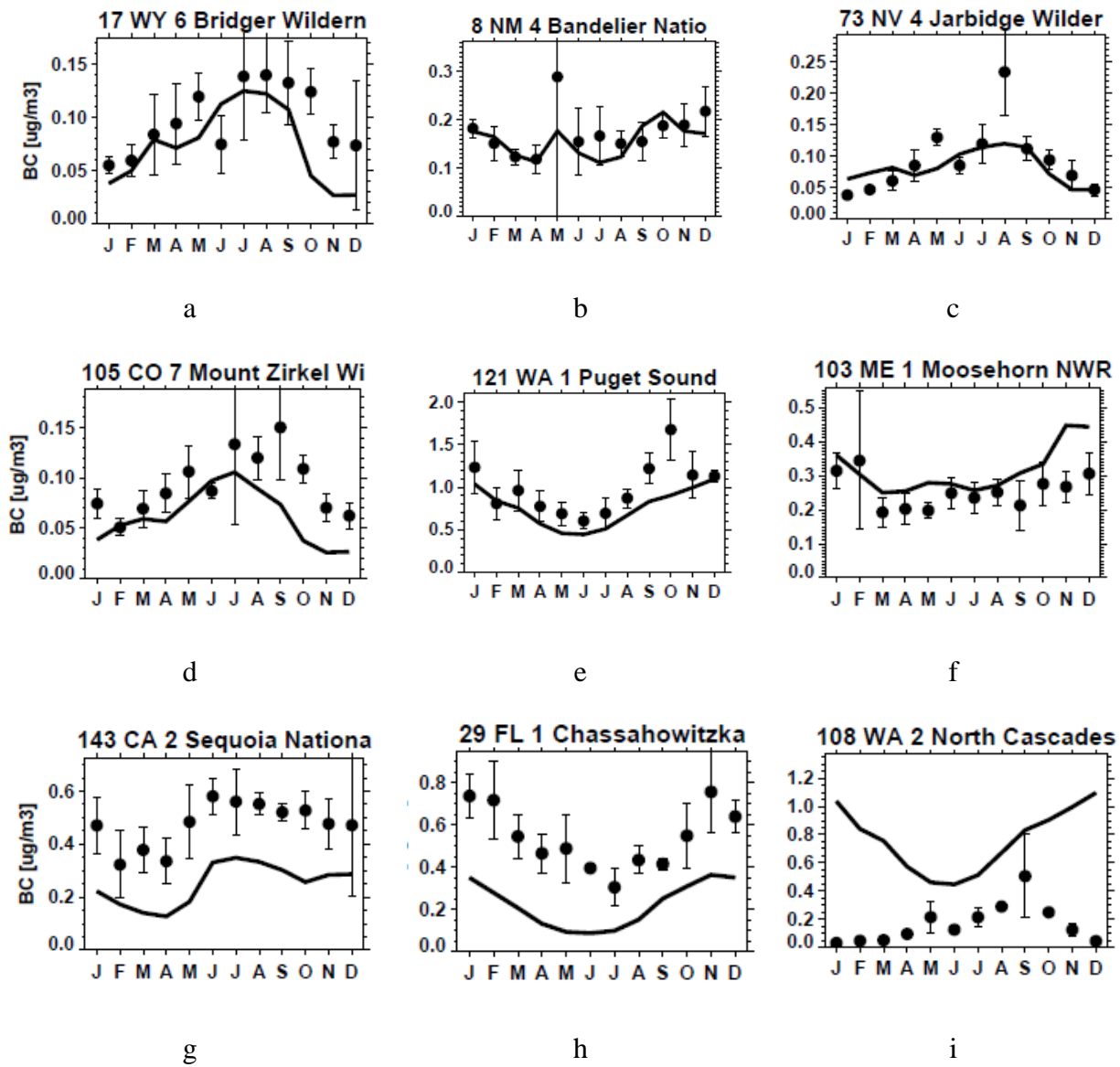


Figure E9 Comparison between simulated and observed monthly BC concentrations (1997-2003 average) over several IMPROVE sites within the United States.

2.2 EMEP observations (EMEP EC/OC campaign 2002-2003):

Figure E10 compares monthly simulated and observed BC concentrations over all EMEP sites participating in the 2002-2003 EC/OC campaign (information for each participating site is given in Table E5). The simulated BC concentrations are in general close to the EMEP observations. However, the model tends to overestimate BC concentrations over Norway, but underestimate BC concentrations over Spain. Again, the bias may come from a bias in biomass burning BC emissions, particularly their seasonal variability in each location.

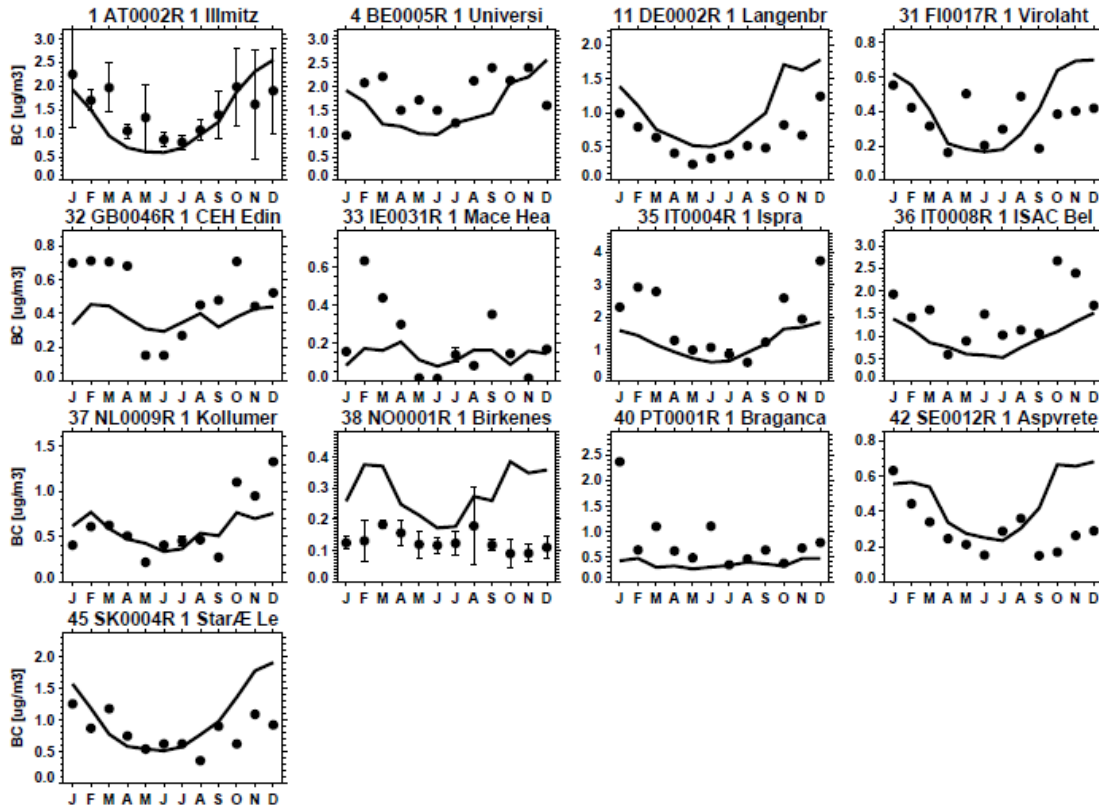


Figure E10 Same as Figure E4, but for EMEP BC observations (Site information can be tracked by site index from Table E5).

Table E5 Information for EMEP observation sites (2002-2003 EC&OC campaign)

Index	Code	Name	Lat	Lon	Height (m)
1	AT0002R	Illmitz	47.76667	16.76667	117
2	AT0004R	St. Koloman	47.65	13.2	851
3	AT0005R	Vorhegg	46.77778	13.02222	1020
4	BE0005R	University of Gent	51.05	3.716667	0
5	CH0002R	Payerne	46.93056	7.047222	489
6	CH0003R	T 鋳 ikon	47.59722	8.947222	539
7	CH0004R	Chaumont	47.19722	7.094444	1137
8	CH0005R	Rigi	47.075	8.588889	1031
9	CZ0003R	Kosetice	49.58333	15.08333	534
10	DE0001R	Westerland	55.00556	8.397222	12
11	DE0002R	Langenbr 黷 ge	52.82222	10.84444	74
12	DE0003R	Schauinsland	48.04722	7.986111	1205
13	DE0004R	Deuselbach	49.89722	7.069444	480
14	DE0005R	Brotjacklriegel	48.84444	13.24167	1016
15	DE0007R	Neuglobsow	53.16667	13.03333	62
16	DE0008R	Schm 黷 ke	50.65	10.76667	937
17	DE0009R	Zingst	54.43333	12.73333	1
18	DE0041R	Westerland Tinnum	54.9	8.333333	481
19	DE0044R	Melpitz	52.65	13.05	86
20	DK0005R	Keldsnor	54.73333	10.73333	10
21	ES0007R	V 韓 nar	37.23333	-3.53333	1265
22	ES0008R	Niembro	43.52222	-4.85278	134
23	ES0009R	Campisabalos	41.41111	-3.22778	1360
24	ES0010R	Cabo de Creus	42.34444	3.319444	23
25	ES0011R	Barcarrola	38.55833	-6.97778	393
26	ES0012R	Zarra	39.11111	-1.11944	885
27	ES0013R	Penausende	41.28333	-5.86667	985
28	ES0014R	Els Torms	41.4	0.716667	470
29	ES0015R	Risco Llamo	39.51667	-4.35	1241
30	ES0016R	O Savi 駟 o	43.36111	-7.84722	506
31	FI0017R	Virolahti II	60.61667	27.71111	4
32	GB0046R	CEH Edingburgh	55.95	-3.21667	0
33	IE0031R	Mace Head	53.16667	-9.5	15
34	IT0001R	Montelibretti	42.1	12.63333	48
35	IT0004R	Ispra	45.8	8.633333	209
36	IT0008R	ISAC Belgona	44.48333	11.33333	0
37	NL0009R	Kollumerwaard	53.33889	6.372222	1

38	N0001R	Birkenes	58.38333	8.25	190
39	N00099R	Lista	58.1	6.566667	13
40	PT0001R	Braganca	41.81667	-6.76667	690
41	SE0011R	Vavihill	56.01667	13.15	175
42	SE0012R	Aspvreten	58.8	17.38333	20
43	SE0035R	Vindeln	64.25	19.76667	225
44	SI0008R	Iskrba	45.56667	14.86667	520
45	SK0004R	Star?Lesn?	49.15	20.28333	808
46	SK0005R	Liesek	49.36667	19.68333	892
47	SK0006R	Starina	49.05	22.26667	345

3. Organic carbon

3.1 IMPROVE observations (1997-2003 average)

As shown in Figure 4c in the paper, the simulated annual mean OC concentrations agree within a factor of 2 with more than 80% of the IMPROVE observations, but tend to be underestimated over a few sites in northern California and the southeastern U.S. (probably due to either the bias in biomass burning emissions or the lack of secondary organic aerosols in this study). In addition, the model overestimates OC concentrations over a few sites in Washington and California (probably due to the bias of biomass burning OC emissions, see Figure E11).

The model captures seasonality in OC concentrations over nearly 55% of IMPROVE sites. Figure E12 shows examples. However, our model tends to systematically underestimate OC concentrations over many sites in the western and southeastern U.S. (see Figure E12g-i), probably due to lack of secondary organic aerosols as well as bias of biomass burning OC emissions.

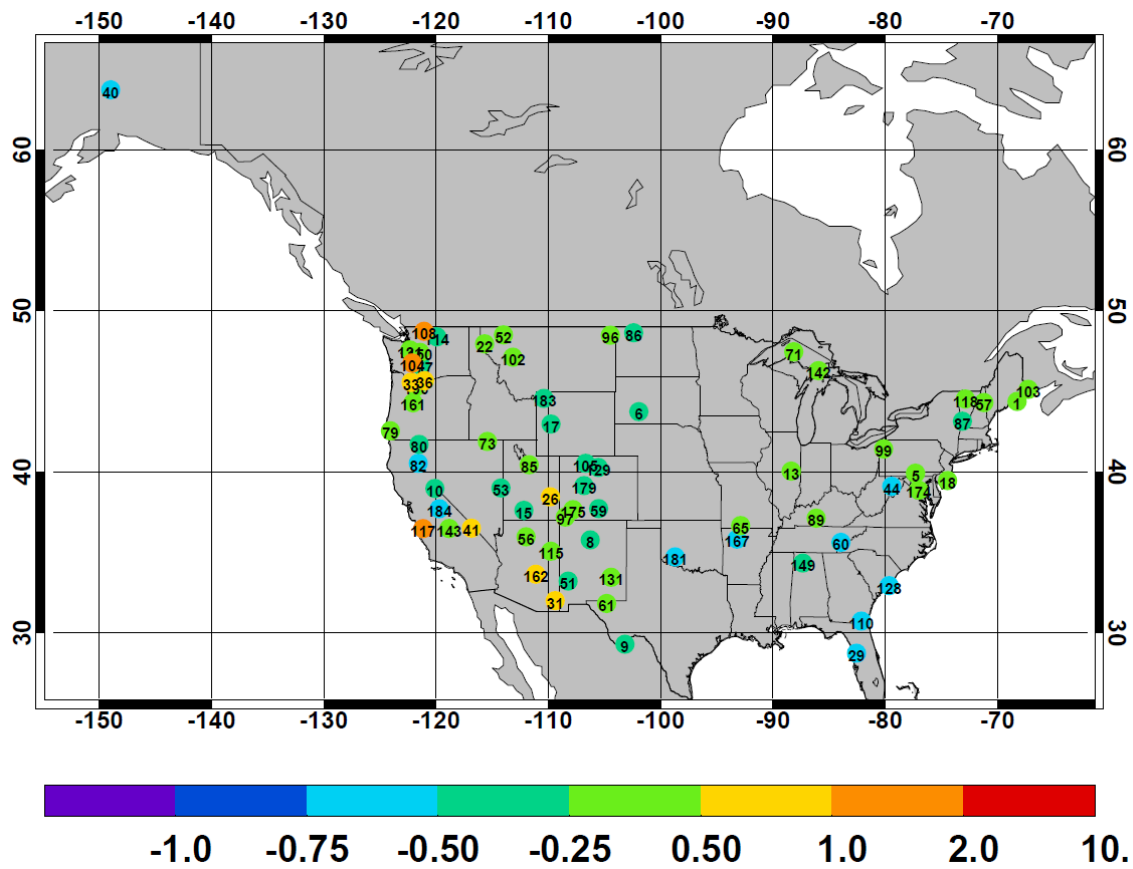


Figure E11 Same as Figure E1, but for organic carbon.

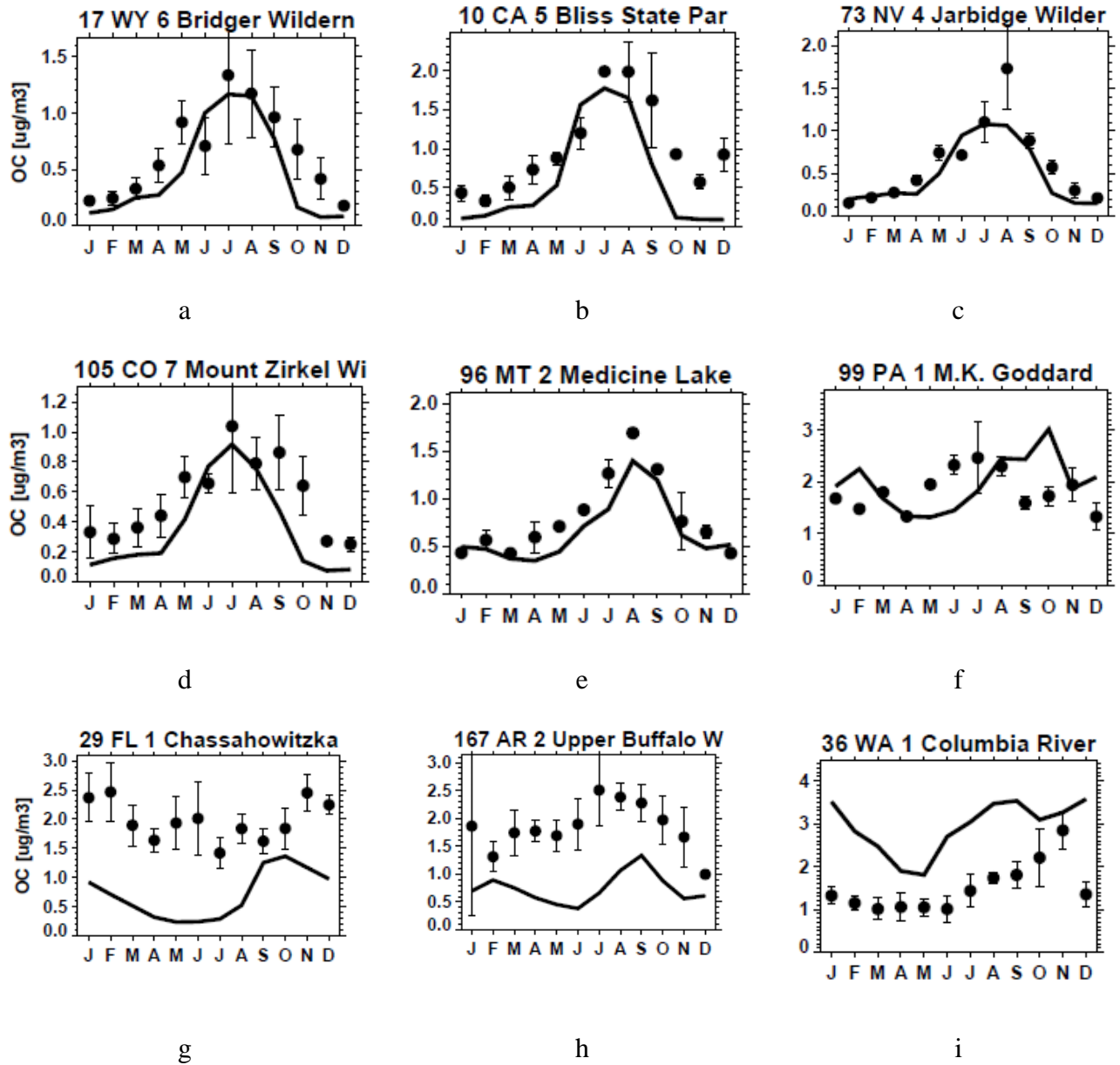


Figure E12 Comparison between simulated and observed monthly OC concentrations (1997-2003 monthly average) over several IMPROVE observation sites.

3.2 EMEP observations (EMEP EC/OC campaign 2002-2003):

Figure E13 lists all the EMEP sites that we used to compare OC simulations. The simulated OC concentrations are generally systematically lower than the EMEP observations by a factor of 1-2. Again, the bias may be caused by both biomass burning emissions as well as a lack of secondary organic aerosols. If we double the simulated OC concentrations to account for the SOA (as suggested by Cooke1999 paper), the magnitude of simulated OC is comparable to the observed EMEP OC (see Figure E14).

From Figure 14, the simulated OC doesn't capture well the seasonal variability, probably due to bias in the seasonal variability of biomass burning emissions as well as the possibility that the seasonal variability of secondary organic aerosols is different than that of anthropogenic and biomass burning OC.

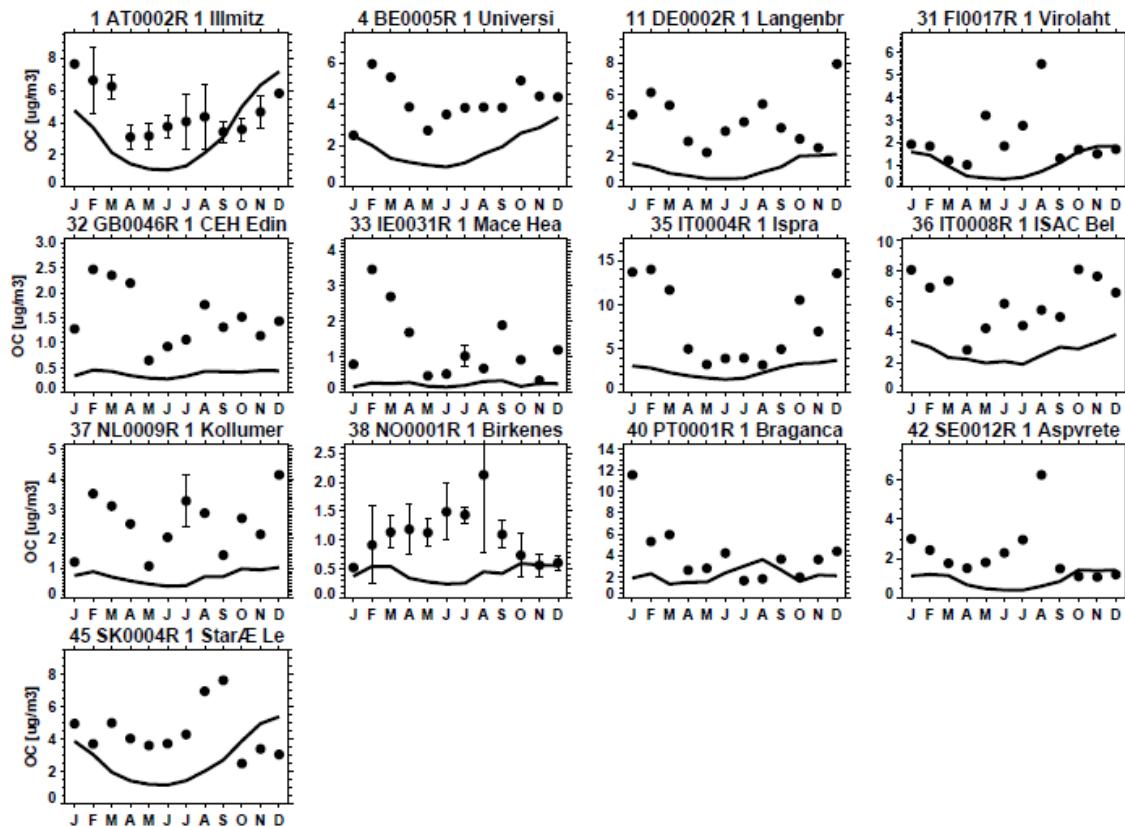


Figure E13 Same as Figure E10, but for EMEP OC observations.

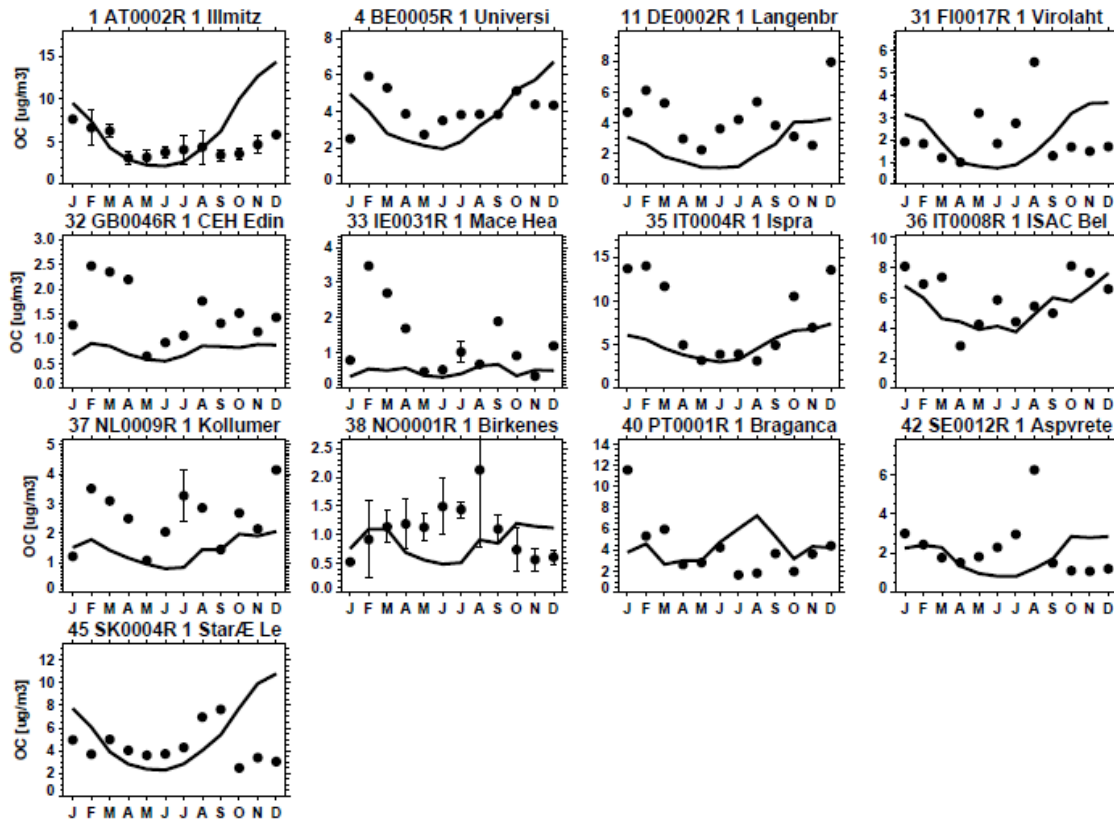


Figure E14 Same as Figure E13, but the simulated OC concentrations are doubled.

4. Dust

4.1 IMPROVE fine dust observations (1997-2003 average)

Figure E15 compares the simulated submicron (with radius 0.1-1 μ m) dust concentrations with IMPROVE observations. Model simulations in general agree within a factor of 2 of the observations and capture well the seasonal cycle of submicron dust concentrations (see Figure E16a-f). However, our model tends to underestimate dust

concentrations over the Southeastern US (particularly in summer, see Figure E16g,h), mostly because the model underestimates trans-Atlantic transport of Saharan dust from North Africa to the southeastern U.S. (also see section 4.2: model comparison to RSMAS data). In contrast, the model tends to systematically overestimate submicron dust concentrations over the desert regions in the western US (see Figure E16i), probably due to the improper treatment of dust emissions over this region.

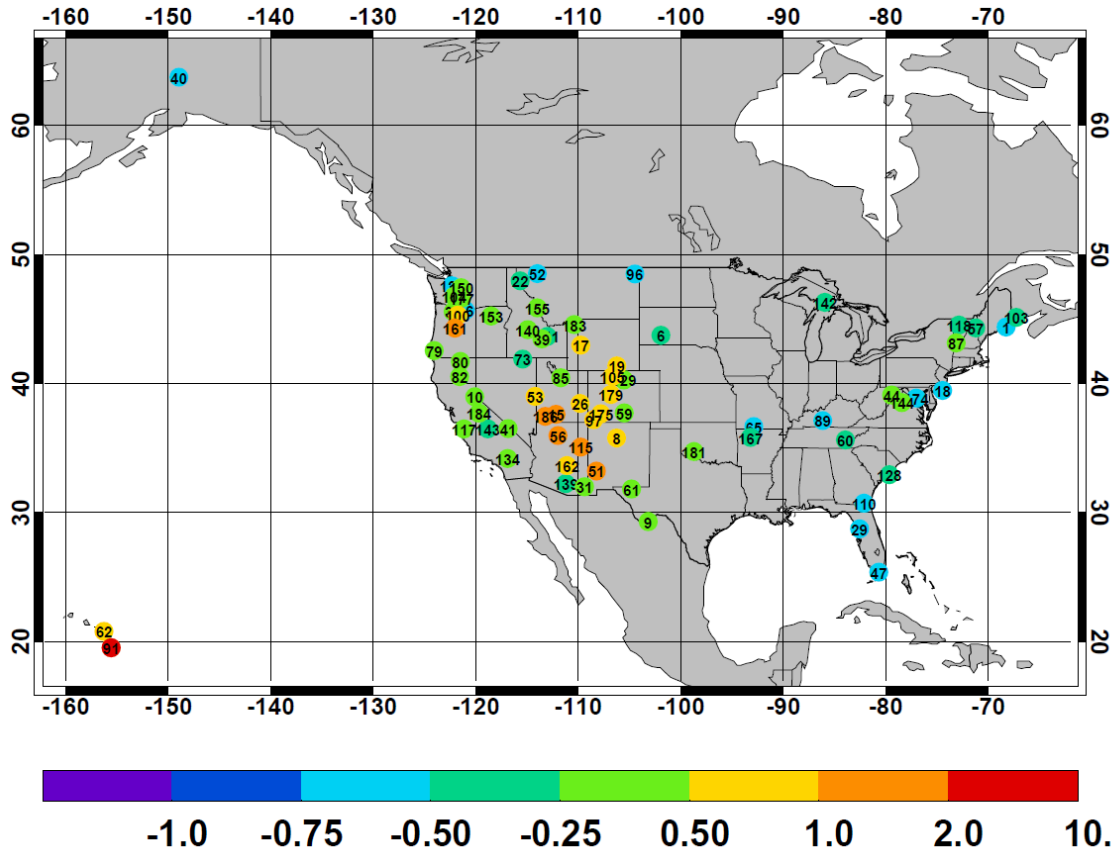


Figure E15 Same as Figure E1, but for IMPROVE dust concentrations.

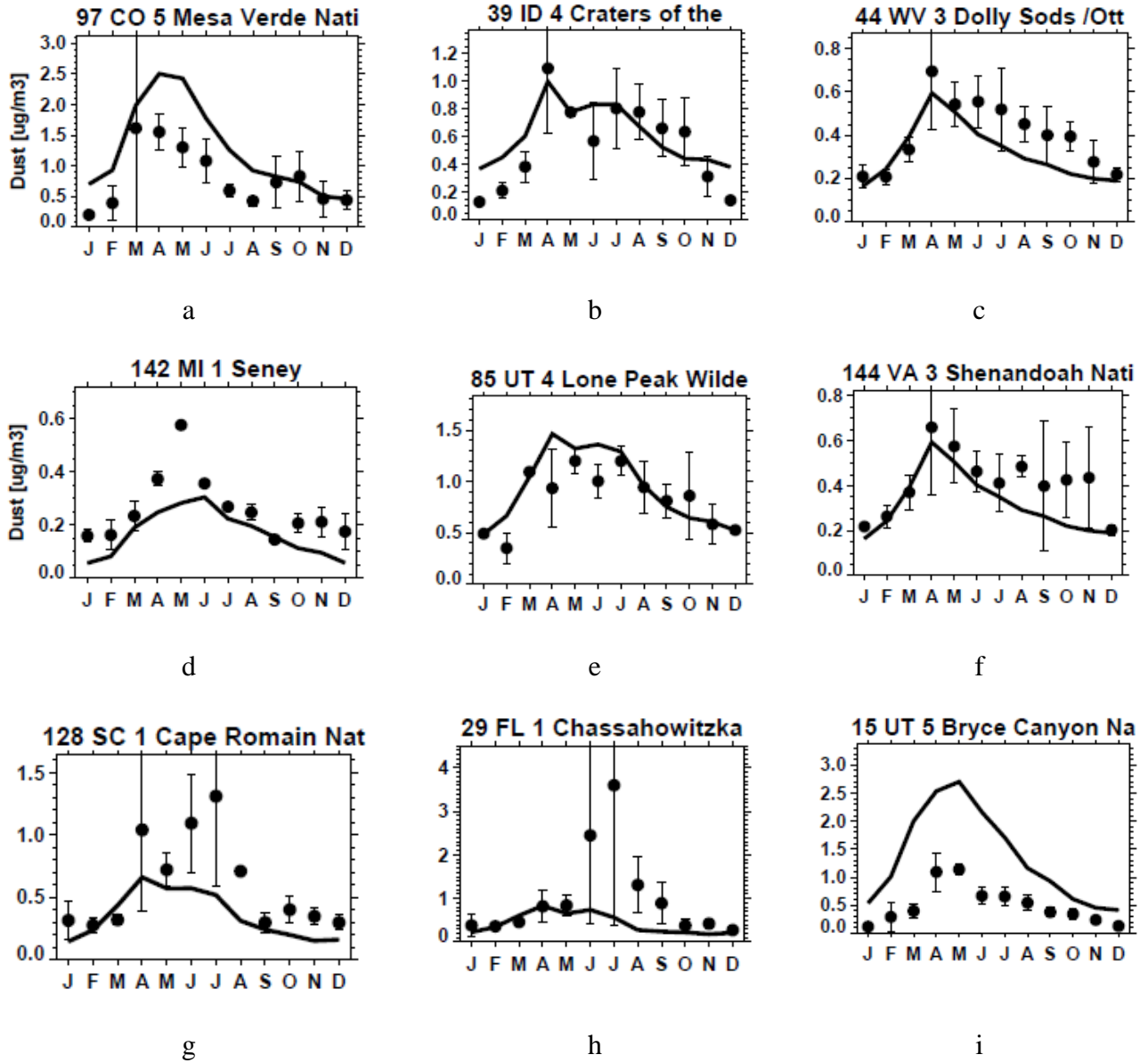


Figure E16 Comparison between simulated and observed monthly submicron dust concentrations (1997-2003 average) over several IMPROVE sites.

4.2 RSMAS observations (1980s-1990s average)

Figure E17 shows the comparison between simulated (1997-2003 average) and observed RSMAS (1980s-1990s average) total dust concentrations. Generally the simulated annual mean dust concentration is close to RSMAS observations over East Asia and Northwest Africa (near the major upwind dust sources). However, the model tends to underestimate summer dust over the western Atlantic and to overestimate summer dust over the tropical Pacific (see Figure E18). Biases may lie in the wet and dry deposition schemes (e.g., the parameterizations of removal rates for different dust size bins) as well as in dust emissions (e.g., in this study we follow Zender, 2003 paper assuming clay fraction of 0.2 in preferential dust sources which are characterized by deposit of alluvium. Future more reliable global erodible soil data will definitely improve our simulations of dust emissions).

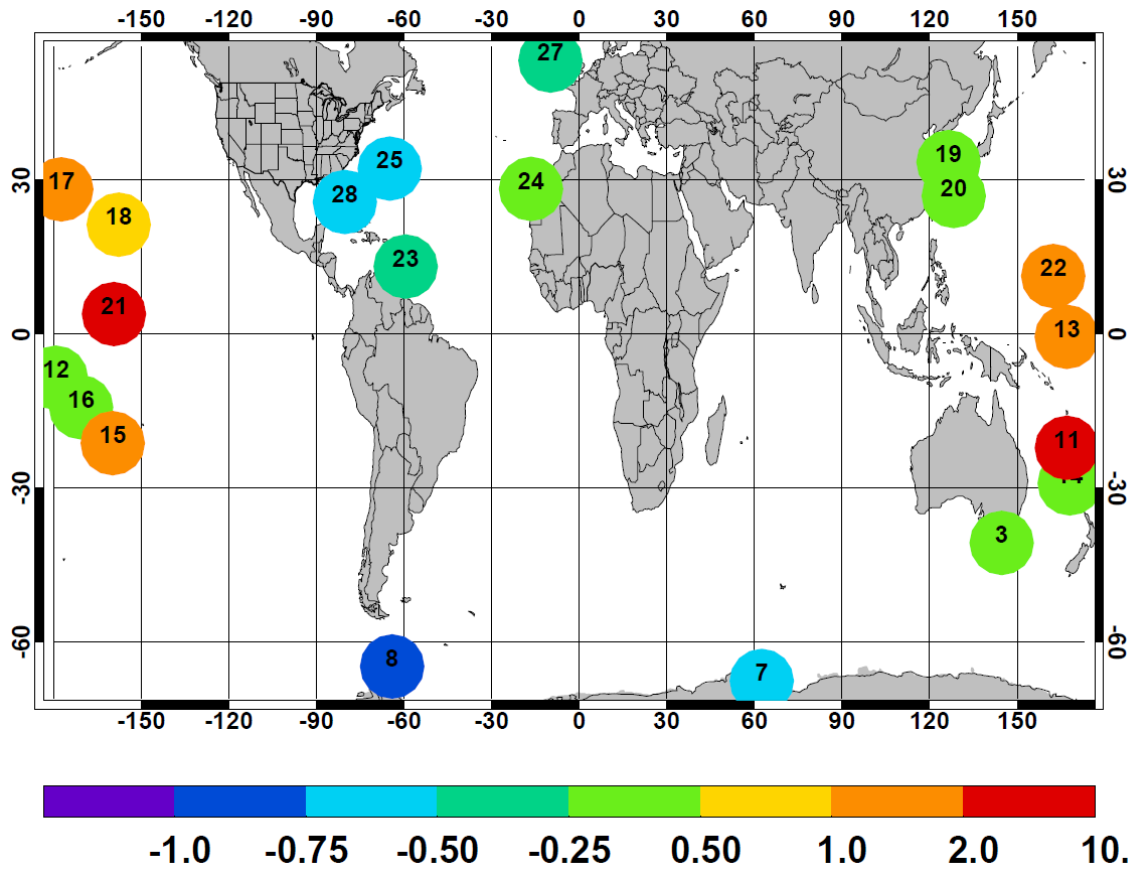


Figure E17 Same as Figure E1, but for RSMAS dust observations (numbers in the circles indicate site index).

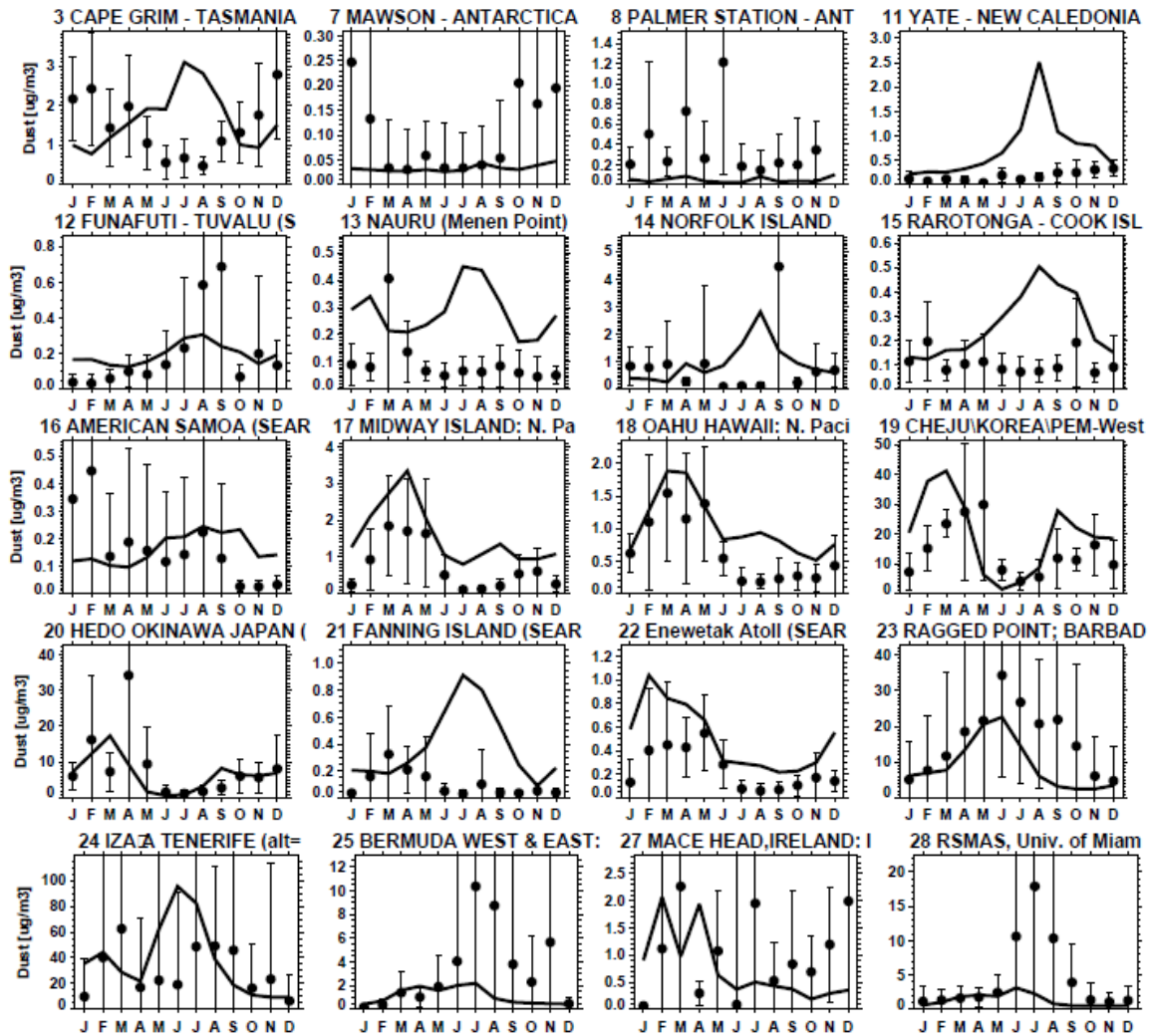


Figure E18 Same as Figure E6, but for RSMAS dust observations.